# 國立交通大學

## 應用數學系數學建模與科學計算碩士班

## 碩 士 論 文

邊界補償法求解熱方程

Stable pseudospectral penalty boundary treatments for heat equations

研究生 :林詩婷

指導教授 :賴明治 博士

共同指導教授 :鄧君豪 博士

中 華 民 國 一百零二 年 六 月

# 邊界補償法求解熱方程

# Stable pseudospectral penalty boundary treatments for heat equations


研 究 生 ：林詩婷　　Student： Shih-Ting Lin

指導教授 ：賴明治　　Advisor： Ming-Chih Lai

共同指導教授 ：鄧君豪　　Co-advisor： Chun-Hao Teng

國立交通大學

應用數學系

數學建模與科學計算碩士班


碩 士 論 文

A Thesis

Submitted to Department of Applied Mathematics College of Science

Institute of Mathematical Modeling and Scientific Computing

National Chiao Tung University

in Partial Fulfillment of the Requirements

for the Degree of

Master

in

Applied Mathematics

June 2013

Hsinchu, Taiwan, Republic of China

中華民國一百零二年六月

# 邊界補償法解熱方程

學生　：林詩婷　　指導教授　：賴明治

共同指導教授　：鄧君豪

國立交通大學

應用數學系

數學建模與科學計算碩士班

摘　要

利用擬譜法並且施加邊界條件逼近熱方程式。在這份論文之中，可以利用離散能量估計確定邊界條件的懲罰參數。我們利用已知正解的齊次熱方程式及非齊次熱方程式做數值計算，並與預期的準確性相符合。

# Stable pseudospectral penalty boundary treatments for heat equations

Student : Shih-Ting Lin
Advisor : Ming-Chih Lai
Co-advisor : Chun-Hao Teng

Institute of Mathematic Modeling and Scientific Computing
Department of Applied Mathematics
National Chiao Tung University
June, 2013

---

**Abstract**

A method to impose boundary conditions for pseudospectral approximations to heat equations is suggested. In this study, the boundary conditions are weakly enforced to the scheme with the penalty parameters which are determined analytically by using the discrete energy estimate. Numerical experiments based on the proposed scheme are performed including homogeneous heat equations and inhomogeneous heat equations where exact solutions exist, and the numerical results show that the accuracy as we expected.

---

# 誌　　謝

本篇論文的完成，首先感謝我的指導老師鄧君豪博士，在這三年間的悉心教誨，讓我一點一滴的了解數值偏微分方程和譜方法，若沒有鄧老師從旁提點，我不會這麼順利的畢業，特別在此獻上我最誠摯的感謝。另外也感謝我的共同指導老師賴明治博士，不僅在課業上諄諄教誨，在生活上亦照顧備至。感謝黃仲尹學長、曾昱豪學長、馮可安學長、陳冠羽學長、胡偉帆學長以及吳聲華學長無私的分享他們知識與經驗，讓此篇論文可以順利完成。

同時感謝我的口試委員洪子倫教授，於口試期間的建議以及對疏漏處的提醒和指正，讓本論文變得更加完備，學生永遠銘記在心。

而在交大的這些日子，無論是在課堂上，亦或是參與各種演講和研討會，都讓我學習到做研究的精神與態度，在此感謝所有我修過課的老師們以及我所參加過的演講的所有教授們。另外我要感謝李金龍老師、莊雅竹同學、王芊惠學姐、廖佳琪學姐、以及所有在大學及碩士期間認識的同學、學長姐和學弟妹，在我的研究生生涯中，因為有你們的陪伴與包容，讓我走過最艱難的日子，忘記過往傷痛，我的生活才得以充實，充滿歡笑與快樂，謝謝你們。再來我要感謝去年我在美國認識的所有人，不論是一起工作的同事或者是一起旅遊的朋友，謝謝你們一直給我加油打氣，也讓我擁有最美好的回憶。

最後，我要好好地感謝我的家人，是他們悉心的照顧與栽培，才會有今日的我。希望能與他們，以及在我身邊所有關心我的人，一起分享這篇論文完成的喜悅與榮耀。

林詩婷 謹致於
交通大學數學建模與科學計算所
中華民國 102 年 6 月

# 目　　錄


中文提要 …… i

英文提要 …… ii

誌謝 …… iii

目錄 …… iv

一、 Introduction …… 1

二、 Formulation …… 3

2.1 Well-posed boundary operator for heat equation …… 3

2.2 Legendre pseudospecctral method: Basic concepts … 4

2.3 Semi-discrete schemes …… 7

2.3.1 One-dimensional problem …… 7

2.3.2 Two-dimensional problem …… 9

2.4 Fully-discrete schemes …… 11

2.5 Direct solver …… 14

三、 Numerical Results …… 15

3.1 One-dimensional problem …… 15

3.2 Two-dimensional problem …… 23

四、 Concluding remarks …… 25

Reference …… 28

Appendix …… 31

A. Stability analysis of one-dimensional semi-discrete schemes …… 31

B. Stability analysis of two-dimensional semi-discrete schemes ..... 32

C. Stability analysis for penalty parameter τ 36

# 1. Introduction

Heat equation is one of the basic partial differential equations. It is of fundamental importance in diverse scientific regions such as physics [2, 12], image analysis [5, 15], financial mathematics [1, 19], and biology [11, 14]. For instance, the diffusion phenomena can be used to describe the change of molecular distribution. In computer graphics, it's useful in de-noise processing of image or filling holes in a certain data. In financial mathematics, the Black-Scholes model can be simplified into the heat equation boundary value problems to discuss the prices change in derivative financial products. In bionomics, the diffusion equations can be representative as the change in the number of species, or the process of gas exchange in protists.

Although heat equations are widely used in various fields, analytic methods for solving partial differential equations are limited, because the problem domain may be complex or the problems may involve non-linearity. Due to the rapid development of computing facility and numerical methods, one may seek approximation solutions to partial differential equations. Hence, how to get accurate and stable numerical results with great efficiency for partial differential equations becomes an important research topic called numerical partial differential equations.

The Lax-Richtmyer equivalent theorem [9] plays a fundamental role in numerical partial differential equations. It states that for a well-posed linear problem the numerical solution obtained by a consistent scheme converges to the exact solutions of the problem if and only if the scheme is stable. Thus, studying the convergence property of a numerical scheme boils down to examining both the consistency and the stability of a scheme. Examining the consistency of a scheme heavily relies on the approximation theory which has been developed for a long time. For example, the Euler scheme for ordinary differential equations has been constructed for more than centuries and the consistency study of the schemes relies on Taylor series expansion. However, the stability theory for numerical schemes are mainly developed since the mid twentieth century. The most fundamental stability theory for numerical scheme is due to von Neumann who proposed a stability analysis in 1944 [13] for periodic problems.

Generally speaking, by exploring the consistency and stability of a scheme, we can

estimate the convergence conditions and the convergence rate in advance. For examples, if we use explicit Euler method [16, 17], we will get second order convergence. We need use more time in the calculation because it is conditionally stable. If using the implicit Euler method [8, 17], this form is unconditionally stable, but it only have first-order convergence accuracy when the grid points are increased. Crank-Nicolson form [4, 17] can reach second-order convergence accuracy and unconditionally stable. However, it needs more grid points by using finite difference method. Hence, requires more computing time on computation inverse matrix is its shortcomings. For this reason, we will focus on how to use less grid points more efficiently to reach the second order convergence accuracy.

In this study, we present a scheme, based on the spectral approximation in space and Crank-Nicolson method in time, for model heat equations defined on square domains subject to various types of boundary conditions. It can be expected that the scheme achieve second order convergence in time. As we know, spectral method can use less grid points to reached the same accuracy as finite different method. So we select the Legendre-Gauss-Labatto grid points [7] for the space discretization. Stable imposing of boundary conditions in spectral methods is very delicate. In this study, boundary conditions are imposed to the scheme through the penalty methodology [6], and we paid special attention to the stability analysis of the scheme based on conducting discrete energy estimates. Though the stability analysis the values of the penalty parameters are found to ensure stable computations. The proposed method is implicit and it requires inverting a matrix to update numerical solution for each time step, which can be expensive. In this study we adopt the eigen-function decomposition approach [3, 10] to efficiently conduct the matrix inversion. Because the matrix size is relatively smaller than finite difference method, and the time step is larger than finite difference method. Hence, cut down the computation time can be achieved.

This thesis is organized as follow. In Section 2, we will introduce the heat equations, domain definition in Cartesian coordinate system, and discuss the stability analysis. In Section 3, we will give detail about the Legendre pseudospectral method, and propose the pseudospectral penalty scheme. Then, we discuss how to determine the penalty conditions. Finally, we present the direct solver for calculation. In Section 4, we give

some basic heat equations example in one-dimension and two-dimension for numerical test. Then, we extend it to more complicated heat equations and compare the differences among different time step, CFL condition, and the number of grid points. Conclusions are given in Section 5.

# 2. Formulation

In this section we first discuss boundary conditions for heat equations.

## 2.1. Well-posed boundary operator for heat equation

Without losing generality we consider the space domain $\Omega \subset \mathbb{R}^2$ with its boundary denoted by $\partial\Omega$. Let $\boldsymbol{x} = (x, y)$ and $t$ be the space and time coordinates, respectively. We consider the function $u(\boldsymbol{x}, t)$ satisfying the initial boundary value problem (IBVP):

$$\frac{\partial u(\boldsymbol{x}, t)}{\partial t} = \nu \nabla^2 u(\boldsymbol{x}, t), \qquad \boldsymbol{x} \in \Omega, t > 0, \tag{1a}$$

$$u(\boldsymbol{x}, 0) = f(\boldsymbol{x}), \qquad \boldsymbol{x} \in \Omega, \tag{1b}$$

$$\mathcal{B}u(\boldsymbol{x}, t) = \alpha(\boldsymbol{x})u + \beta(\boldsymbol{x})\frac{\partial u}{\partial n} = g(t), \qquad \boldsymbol{x} \in \partial\Omega, t > 0, \tag{1c}$$

where $\nu > 0$ is the diffusion constant, $\nabla^2$ is the Laplace operator, $f$ is the initial profile of $u$, and $\mathcal{B}u = g$ is the boundary condition imposed at the domain boundary. The symbol $\mathcal{B}$ is the term of the boundary operator which is parameterized by non-negative smooth functions $\alpha(\boldsymbol{x})$ and $\beta(\boldsymbol{x})$ satisfying the constrain $\alpha^2(\boldsymbol{x}) + \beta^2(\boldsymbol{x}) \neq 0$ on $\partial\Omega$. The notation $\partial u/\partial n$ is the usual normal derivative of $u$ on the domain boundary.

Consider homogeneous boundary condition, that is, $g(t) = 0$. Assuming that there exists an unique solution to the IBVP, one can easily obtain an energy rate equation for the described IBVP as follows. Multiplying $u$ to Eq. (1a), integrating over the domain $\Omega$, invoking the divergence theorem, and applying the boundary condition, one obtains

$$\begin{aligned} \frac{1}{2}\frac{d}{dt}\int_\Omega u^2 d\boldsymbol{x} &= -\nu \oint_\Omega \frac{\alpha}{\beta} u^2 d\boldsymbol{x} - \nu \int_\Omega |\nabla u|^2 \, d\boldsymbol{x} \\ &\leq 0 \end{aligned}$$

provided that $\beta \neq 0$. Notice that if the boundary condition is of Dirichlet or Neumann kind then the boundary integration term vanishes. Thus, integrating the above expression

with respect to time and applying the initial condition lead to an energy bound for $u$ at any given time $t > 0$ as

$$\int_\Omega u^2(\boldsymbol{x}, t) d\boldsymbol{x} \leq \int_\Omega f^2(\boldsymbol{x}) d\boldsymbol{x}.$$

Therefore, the problem is well-posed.

Since our concern is about constructing stable imposition of boundary condition for numerical computations, we consider the problem defined $\Omega = [-1, 1]^2$ for simplicity. The problem becomes

$$\frac{\partial}{\partial t} u(x, y, t) = \nu \nabla^2 u(x, y, t), \qquad (x, y) \in \Omega, t > 0 \tag{2a}$$

$$u(x, y, 0) = f(x, y), \qquad (x, y) \in \Omega, \tag{2b}$$

$$\mathcal{B}^{(a)} u(-1, y, t) = g_-(y, t), \quad \mathcal{B}^{(a)} = \alpha^{(a)} - \beta^{(a)} \frac{\partial}{\partial x}, \qquad y \in [-1, 1], t > 0. \tag{2c}$$

$$\mathcal{B}^{(b)} u(+1, y, t) = g_+(y, t), \quad \mathcal{B}^{(b)} = \alpha^{(b)} + \beta^{(b)} \frac{\partial}{\partial x}, \qquad y \in [-1, 1], t > 0. \tag{2d}$$

$$\mathcal{B}^{(c)} u(x, -1, t) = h_-(x, t), \quad \mathcal{B}^{(c)} = \alpha^{(c)} - \beta^{(c)} \frac{\partial}{\partial y}, \qquad x \in [-1, 1], t > 0. \tag{2e}$$

$$\mathcal{B}^{(d)} u(x, +1, t) = h_+(x, t), \quad \mathcal{B}^{(d)} = \alpha^{(d)} + \beta^{(d)} \frac{\partial}{\partial y}, \qquad x \in [-1, 1], t > 0. \tag{2f}$$

The symbols $\mathcal{B}^{(\gamma)}$ for $\gamma \in \{a, b, c, d\}$ are the boundary operators defined on the edges of the square domain. Along each edge, the associated boundary operator is parameterized by a pair of constant real numbers, $\alpha^{(\gamma)} \geq 0$ and $\beta^{(\gamma)} \geq 0$, satisfying the constrain $(\alpha^{(\gamma)})^2 + (\beta^{(\gamma)})^2 \neq 0$.

Later in this report, we propose pseudospectral schemes with stable imposition of boundary conditions for the problem described by Eqs. (2a)-(2f).

## 2.2. Legendre pseudospectral method: Basic concepts

Consider the interval $\mathsf{I} = [-1, 1]$. Let $N$ be a positive integer. Denoted by $x_i$, for $i = 0, 1, \cdots, N$, the Legendre-Gauss-Lobatto (LGL) points ordered increasingly as $-1 = x_0 < x_1 < \cdots < x_N = 1$, are roots of the polynomial $Q(x) = (1 - x^2) P'_N(x)$, where $P_N(x)$ is the Legendre polynomial of degree $N$ and $'$ denotes the differentiation.

Based on LGL points, we can construct the Lagrange interpolation basis functions

$l_j(x)$ as

$$l_j(x) = \frac{Q(x)}{(x - x_j)Q'(x_j)} = \frac{-1}{N(N+1)} \frac{(1-x^2)P'_N(x)}{(x - x_j)P_N(x_j)}, \quad j = 0, 1, \cdots, N,$$

satisfying the property:

$$l_j(x_i) = \begin{cases} 0, & \text{if } i \neq j \\ 1, & \text{if } i = j \end{cases}.$$

For a function $f(x)$ defined on $x \in \mathsf{I}$, we can approximate $f(x)$ and its $p$-th derivative as follows,

$$f(x) \approx f_N(x) = \sum_{j=0}^{N} l_j(x) f(x_j), \quad f^{(p)}(x_i) \approx f_N^{(p)}(x_i) = \sum_{j=0}^{N} \frac{d^p l_j(x_i)}{dx^p} f(x_j).$$

The numerical derivatives can be computed through a matrix-vector multiplication,

$$\boldsymbol{f}^{(p)} = \boldsymbol{D}^p \boldsymbol{f},$$

where $\boldsymbol{f}^{(p)}$ and $\boldsymbol{f}$ are vectors given as

$$\boldsymbol{f}^{(p)} = \left[ f_N^{(p)}(x_0), f_N^{(p)}(x_1), \cdots, f_N^{(p)}(x_N) \right]^T,$$
$$\boldsymbol{f} = \left[ f_N(x_0), f_N(x_1), \cdots, f_N(x_N) \right]^T,$$

with $T$ being the vector transpose, and $\boldsymbol{D}$ is call the differential matrix with entries given as $D_{ij} = l'_j(x_i)$. The values of $l'_j(x_i)$ can be found in [7].

For each $N$, the set of LGL points is associated with a set of quadrature weights $\{\omega_i\}_{i=0}^N$ such that

$$\sum_{i=0}^{N} f(x_i)\omega_i = \int_{-1}^{1} f(x)dx, \tag{3}$$

provided that $f(x)$ being a polynomial of degree at most $2N - 1$. Equation (3) is also known as the LGL integration quadrature rule, and it leads to the following result. Let $u$ and $v$ both be polynomials of degree at most $N$. Then $uv'$ is a polynomial of degree at most $2N - 1$, and we have

$$\sum_{i=0}^{N} u(x_i)v'(x_i)\omega_i = u(x_N)v(x_N) - u(x_0)v(x_0) - \sum_{i=0}^{N} u'(x_i)v(x_i)\omega_i, \tag{4}$$

followed by the quadrature rule. Equation (4) is the discrete analog of the integration-by-parts rule $\int_{-1}^{1} uv'dx = uv|_{-1}^{1} - \int_{-1}^{1} vu'dx$. We will later use this formula to establish the stability of the proposed schemes for heat equations.

Employing the tensor product formulation, we can extend the above one-dimensional concepts to approximate functions defined on the two dimensional domain $\mathsf{I}^2 = [-1, 1]^2$. Define the two-dimensional collocation points as

$$\boldsymbol{x}_{ij} = (x_i, y_j), \quad 0 \le i \le M, \quad 0 \le j \le N,$$

where $x_i$ and $y_j$ are the LGL points along $x$ and $y$ axes, respectively. The two-dimensional Lagrange basis polynomials, based on the grid points $(x_i, y_j)$, are constructed as

$$L_{ij}(x, y) = l_i^x(x) l_j^y(y),$$

where $l_i^x(x)$ and $l_j^y(y)$ are the one-dimensional Lagrange interpolation polynomials based on $x_i$ and $y_j$, respectively. Thus, we can approximate a function $f(\boldsymbol{x})$ defined on $\mathsf{I}^2$ as

$$f(x, y) \approx f_{MN}(x, y) = \sum_{ij}^{MN} L_{ij}(x, y) f(x_i, y_j), \quad \sum_{ij}^{MN} = \sum_{j=0}^{N} \sum_{i=0}^{M},$$

where we have used $\sum_{ij}^{MN}$ as a shorthand notation of $\sum_{j=0}^{N} \sum_{i=0}^{M}$. The partial derivatives of $f$ at a grid point $(x_i, y_j)$ are approximated as

$$\frac{\partial f(x_i, y_j)}{\partial x} \approx \frac{\partial f_{MN}(x_i, y_j)}{\partial x} = \sum_{i'j'}^{MN} \frac{\partial L_{i'j'}(x_i, y_j)}{\partial x} f(x_{i'}, y_{j'}),$$

$$\frac{\partial f(x_i, y_j)}{\partial y} \approx \frac{\partial f_{MN}(x_i, y_j)}{\partial y} = \sum_{i'j'}^{MN} \frac{\partial L_{i'j'}(x_i, y_j)}{\partial y} f(x_{i'}, y_{j'}).$$

The numerical derivatives can be evaluated through a matrix-vector multiplication as follows,

$$\boldsymbol{F}_x = \boldsymbol{D}_x \boldsymbol{F}, \quad \boldsymbol{F}_y = \boldsymbol{F} \boldsymbol{D}_y^T,$$

where $\boldsymbol{F}$ is a $(M+1) \times (N+1)$ matrix with entries being $F_{ij} = f(x_i, y_j)$, $\boldsymbol{D}_x$ and $\boldsymbol{D}_y$ are the $(M+1) \times (M+1)$ and $(N+1) \times (N+1)$ differentiation matrices in $x$- and $y$-directions, respectively, and $\boldsymbol{F}_x$ and $\boldsymbol{F}_y$ are the matrices whose elements are the numerical partial derivatives $\partial f_{MN}(x_i, y_j)/\partial x$ and $\partial f_{MN}(x_i, y_j)/\partial y$, respectively.

The one dimensional quadrature rule, Eq. (3), can be applied dimension by dimension to conduct discrete integration-by-parts of functions defined on $\mathsf{I}^2$. Define the two-dimensional LGL quadrature weights as $\omega_{ij} = \omega_i^x \omega_j^y$ where $\omega_i^x$ and $\omega_j^y$ are the quadrature weights associated with the LGL points $x_i$ and $y_j$, respectively. Let $u(x, y)$ and $v(x, y)$ both be polynomials of degree at most $M$ and $N$ in $x$ and $y$, respectively. For simplicity we denote $u_{ij} = u(x_i, y_j)$ and $v_{ij} = v(x_i, y_j)$. Then, we have

$$\sum_{ij}^{MN} \left( u \frac{\partial v}{\partial x} \omega \right) \Bigg|_{ij} = \sum_{j=0}^{N} \left[ (uv)|_{Mj} - (uv)|_{0j} \right] \omega_j^y - \sum_{ij}^{MN} \left( \frac{\partial u}{\partial x} v \omega \right) \Bigg|_{ij}, \tag{5a}$$

$$\sum_{ij}^{MN} \left( u \frac{\partial v}{\partial y} \omega \right) \Bigg|_{ij} = \sum_{j=0}^{N} \left[ (uv)|_{iN} - (uv)|_{i0} \right] \omega_i^x - \sum_{ij}^{MN} \left( \frac{\partial u}{\partial y} v \omega \right) \Bigg|_{ij}. \tag{5b}$$

For further concepts of the Legendre pseudospectral methods, we refer the reader to [7].

## 2.3. Semi-discrete schemes

We now present the semi-discrete numerical schemes for the heat equations defined on one- and two-dimensional spaces. The conceptual ideas of the methods will be demonstrated through the one-dimensional problem in details. The two-dimensional schemes will be extended from the one-dimensional schemes through a tensor product formulation.

### 2.3.1. One-dimension problem

Let us consider the one dimension problem:

$$\begin{aligned}
\frac{\partial u(x,t)}{\partial t} &= \nu \frac{\partial u^2(x,t)}{\partial x^2}, && x \in \mathsf{I}, t > 0, \\
u(x,0) &= f(x), && x \in \mathsf{I}, \\
\mathcal{B}_+ u(+1,t) &= \alpha_+ u(+1,t) + \beta_+ \frac{\partial u(+1,t)}{\partial x} = g_+(t), && t > 0, \\
\mathcal{B}_- u(-1,t) &= \alpha_- u(-1,t) - \beta_- \frac{\partial u(-1,t)}{\partial x} = g_-(t), && t > 0.
\end{aligned}$$

We introduce $N + 1$ LGL grid points on $\mathsf{I}$. Let $v_j(t)$ be the collocated field values at the LGL grid points $x_j$. To numerically solve the problem we seek a numerical solution $v(x, t)$ of the form.

$$v(x,t) = \sum_{j=0}^{N} l_j(x) v_j(t), \tag{6}$$

satisfying the collocation equations

$$\frac{\partial v(x_i,t)}{\partial t} = \nu \frac{\partial F(x_i,t)}{\partial x}, \qquad i = 0,1,...,N, \tag{7a}$$

$$v(x_i,0) = f(x_i), \qquad i = 0,1,...,N, \tag{7b}$$

where $F(x,t)$ is given as

$$F(x,t) = \frac{\partial v(x,t)}{\partial x} + \tau_- l_0(x)\left(\mathcal{B}_- v_0 - g_-(t)\right) - \tau_+ l_N(x)\left(\mathcal{B}_+ v_N - g_+(t)\right), \tag{7c}$$

with

$$\mathcal{B}_- v_0 = \alpha_- v(-1,t) - \beta_- \frac{\partial v(-1,t)}{\partial x}, \quad \mathcal{B}_+ v_N = \alpha_+ v(+1,t) + \beta_+ \frac{\partial v(+1,t)}{\partial x}.$$

The present approach of imposing boundary condition follows the method in [18] for second-order wave equations. In the above expression, the boundary conditions are weakly enforced to the scheme, and we have introduced two free penalty parameters $\tau_-$ and $\tau_+$. The values of these parameters will be determined later such that the scheme is stable, in the sense that the scheme has a bounded energy estimate.

We now proceed on determining the values of $\tau_-$ and $\tau_+$ such that the scheme is stable. For stability analysis, it is sufficient to consider homogeneous boundary conditions, that is, $g_\pm(t) = 0$. Multiplying Eq. (7a) by $\nu^{-1} v_i \omega_i$ and summing over the index $i = 0$ to $N$, we have the energy rate equation of the form

$$\frac{1}{2\nu}\frac{d}{dt}\sum_{i=0}^{N} v_i^2 \omega_i = \sum_{i=0}^{N} \omega_i v_i \frac{\partial F(x_i,t)}{\partial x}. \tag{8}$$

Since $v(x_i,t)(\partial F(x_i,t)/\partial x)$ are values of the polynomial $v(x,t)(\partial F(x,t)/\partial x)$ which is of degree at most $2N-1$ in $x$, we invoke the LGL quadrature rule, Eq. (3), to evaluate the discrete summation on the right hand side of Eq. (8). The result is given as follows

$$\begin{aligned}\sum_{i=0}^{N}\left(\omega v \frac{\partial F}{\partial x}\right)\Bigg|_i =& v_N \frac{\partial v_N}{\partial x} - v_0 \frac{\partial v_0}{\partial x} - \sum_{i=0}^{N} \omega_i \left(\frac{\partial v_i}{\partial x}\right)^2 \\ & - \alpha_- \tau_- v_0^2 + \left(\beta_- \tau_- - \alpha_- \tau_- \omega_0\right) v_0 \frac{\partial v_0}{\partial x} + \beta_- \tau_- \omega_0 \left(\frac{\partial v_0}{\partial x}\right)^2 \\ & - \alpha_+ \tau_+ v_N^2 - \left(\beta_+ \tau_+ - \alpha_+ \tau_+ \omega_N\right) v_N \frac{\partial v_N}{\partial x} + \beta_+ \tau_+ \omega_N \left(\frac{\partial v_N}{\partial x}\right)^2.\end{aligned}$$

Define a vector function $\boldsymbol{V}$ and a matrix function $\boldsymbol{A}$ as follows,

$$\boldsymbol{V}(V_1, V_2) = (V_1,\ V_2)^T, \quad \boldsymbol{A}(\alpha, \beta, \tau, \omega) = \begin{pmatrix} -2\alpha\tau & 1 + \alpha\tau\omega - \beta\tau \\ 1 + \alpha\tau\omega - \beta\tau & -2\omega(1 - \beta\tau) \end{pmatrix}. \tag{9}$$

Let

$$\boldsymbol{V}_- = \boldsymbol{V}(v_0, -\partial v_0/\partial x), \quad \boldsymbol{V}_+ = \boldsymbol{V}(v_N, \partial v_N/\partial x), \quad \boldsymbol{A}_\pm = \boldsymbol{A}(\alpha_\pm, \beta_\pm, \tau_\pm, \bar{\omega}), \tag{10}$$

with $\bar{\omega} = \frac{2}{N(N+1)}$. The energy rate equation can be further expressed as

$$\nu^{-1}\frac{d}{dt}\sum_{i=0}^{N} v_i^2\omega_i = \boldsymbol{V}_-^T\boldsymbol{A}_-\boldsymbol{V}_- + \boldsymbol{V}_+^T\boldsymbol{A}_+\boldsymbol{V}_+ - 2\sum_{i=1}^{N-1}\left(\frac{\partial v_i}{\partial x}\right)^2\omega_i,$$

The detail of derivation can be found in Appendix A. For stability, we require

$$\frac{d}{dt}\sum_{i=0}^{N} v_i^2\omega_i \le 0.$$

Thus, a sufficient condition for stability is that the quadratic terms, $\boldsymbol{V}_+^T\boldsymbol{A}_+\boldsymbol{V}_+$ and $\boldsymbol{V}_-^T\boldsymbol{A}_-\boldsymbol{V}_-$, are non-positive. Hence, we are led to find the value of $\tau_\pm$ such that the eigenvalues of $\boldsymbol{A}_\pm$ are non-positive. A simply computation (in Appendix C) reveals that

$$\tau_\pm = \frac{1}{\alpha_\pm\bar{\omega} + \beta_\pm} \tag{11}$$

ensures the desired property.

### 2.3.2. Two-dimensional problem

We can apply a similar approach to construct a pseudospectral scheme for the IBVP described by Eqs. (2a)-(2f). Introduce the two dimensional LGL grid points $(x_i, y_j)$ on $\mathsf{I}$. Let $v_{ij}(t)$ be the collocated field values at the grid points. We seek a numerical solution $v(x, y, t)$ of the form

$$v(x, y, t) = \sum_{i'j'}^{MN} L_{i'j'}(x, y)v_{i'j'}(t),$$

satisfying the semi-discrete scheme:

$$\frac{1}{\nu}\frac{\partial v_{ij}(t)}{\partial t} = \frac{\partial F_x(x_i, y_j, t)}{\partial x} + \frac{\partial F_y(x_i, y_j, t)}{\partial y}, \qquad 0 \le i \le M,\ 0 \le j \le N, \tag{12a}$$

$$v_{ij}(0) = f(x_i, y_j), \qquad 0 \le i \le M,\ 0 \le j \le N, \tag{12b}$$

with

$$F_x(x,y,t) = \frac{\partial v(x,y,t)}{\partial x} + \sum_{j'=0}^{N} \tau^{(a)} L_{0j'}(x,y) \left( \mathcal{B}^{(a)} v_{0j'}(t) - g_-(y_{j'},t) \right) - \sum_{j'=0}^{N} \tau^{(b)} L_{Mj'}(x,y) \left( \mathcal{B}^{(b)} v_{Mj'}(t) - g_+(y_{j'},t) \right), \tag{12c}$$

$$F_y(x,y,t) = \frac{\partial v(x,y,t)}{\partial y} + \sum_{i'=0}^{M} \tau^{(c)} L_{i'0}(x,y) \left( \mathcal{B}^{(c)} v_{i'0}(t) - h_-(x_{i'},t) \right) - \sum_{i'=0}^{M} \tau^{(d)} L_{i'N}(x,y) \left( \mathcal{B}^{(d)} v_{i'N}(t) - h_+(x_{i'},t) \right), \tag{12d}$$

Notice that $\tau^{(a)}$, $\tau^{(b)}$, $\tau^{(c)}$, and $\tau^{(d)}$ are the penalty parameters associated with the edges, and their values will be determined such that the scheme is stable.

For stability analysis, it is sufficient to consider the problem subject to homogeneous boundary conditions, that is, $g_\pm(y,t) = 0$ and $h_\pm(x,t) = 0$. Multiplying $v_{ij}\omega_{ij}$ to Eq. (12a) and summing all resultant collocation equations, we have the energy rate equation

$$\frac{1}{2\nu}\frac{d}{dt}\sum_{ij}^{MN}(v^2\omega)|_{ij} = \sum_{ij}^{MN}\left(\omega v\frac{\partial F_x}{\partial x}\right)\Big|_{ij} + \sum_{ij}^{MN}\left(\omega v\frac{\partial F_y}{\partial y}\right)\Big|_{ij}, \tag{13}$$

Notice that $v\frac{\partial F_x}{\partial x}$ is a polynomial of degree at most $2M-1$ in $x$ for a fixed $y_j$ and $v\frac{\partial F_y}{\partial y}$ is a polynomial of degree at most $2N-1$ in $y$ for a fixed $x_i$. Hence, we can use Eqs. (5a) and (5b) to evaluate the discrete summations on the right hand side of Eq. (13) as follows

$$\sum_{ij}^{MN}\left(\omega v\frac{\partial F_x}{\partial x}\right)\Big|_{ij} = \frac{1}{2}\sum_{j=0}^{N}\omega_j^y(\boldsymbol{V}_j^{(a)})^T\boldsymbol{A}^{(a)}\boldsymbol{V}_j^{(a)} + \frac{1}{2}\sum_{j=0}^{N}\omega_j^y(\boldsymbol{V}_j^{(b)})^T\boldsymbol{A}^{(b)}\boldsymbol{V}_j^{(b)} - \sum_{j=0}^{N}\sum_{i=1}^{M-1}\omega_{ij}\left(\frac{\partial v}{\partial x}\right)^2\Big|_{ij},$$

$$\sum_{ij}^{MN}\left(\omega v\frac{\partial F_y}{\partial y}\right)\Big|_{ij} = \frac{1}{2}\sum_{i=0}^{M}\omega_i^x(\boldsymbol{V}_i^{(c)})^T\boldsymbol{A}^{(c)}\boldsymbol{V}_i^{(c)} + \frac{1}{2}\sum_{i=0}^{M}\omega_i^x(\boldsymbol{V}_i^{(d)})^T\boldsymbol{A}^{(d)}\boldsymbol{V}_i^{(d)} - \sum_{j=0}^{N}\sum_{i=1}^{M-1}\omega_{ij}\left(\frac{\partial v}{\partial x}\right)^2\Big|_{ij},$$

where through Eq. (9)

$$\boldsymbol{V}_j^{(a)} = \boldsymbol{V}(v_{0j}, -(\partial v_{0j}/\partial x)), \quad \boldsymbol{V}_j^{(b)} = \boldsymbol{V}(v_{Mj}, \partial v_{Mj}/\partial x), \tag{14a}$$

$$\boldsymbol{V}_i^{(c)} = \boldsymbol{V}(v_{i0}, -(\partial v_{i0}/\partial y)), \quad \boldsymbol{V}_i^{(d)} = \boldsymbol{V}(v_{iN}, \partial v_{iN}/\partial y), \tag{14b}$$

and for $\gamma$ =a, b, c, and d

$$\boldsymbol{A}^{(\gamma)} = \boldsymbol{A}(\alpha^{(\gamma)}, \beta^{(\gamma)}, \tau^{(\gamma)}, \omega^{(\gamma)}), \quad \omega^{(\gamma)} = \begin{cases} \frac{2}{M(M+1)} & \text{if } \gamma = a, b \\ \frac{2}{N(N+1)} & \text{if } \gamma = c, d \end{cases}. \tag{14c}$$

Thus, Eq. (13) can be written as

$$\frac{1}{\nu}\frac{d}{dt}\sum_{ij}^{MN}(v^2\omega)|_{ij} \leq \sum_{j=0}^{N}\omega_j^y(\boldsymbol{V}^{(a)})_j^T\boldsymbol{A}^{(a)}\boldsymbol{V}_j^{(a)} + \sum_{j=0}^{N}\omega_j^y(\boldsymbol{V}^{(b)})_j^T\boldsymbol{A}^{(b)}\boldsymbol{V}_j^{(b)} + \sum_{i=0}^{M}\omega_i^x(\boldsymbol{V}^{(c)})_i^T\boldsymbol{A}^{(c)}\boldsymbol{V}_i^{(c)} + \sum_{i=0}^{M}\omega_i^x(\boldsymbol{V}^{(d)})_i^T\boldsymbol{A}^{(d)}\boldsymbol{V}_i^{(d)}.$$

The detail of derivation can be found in Appendix B. Similarly, if the eigenvalues of $\boldsymbol{A}^{(\gamma)}$ are non-positive, the scheme is stable. Immediately, we have

$$\tau^{(\gamma)} = \frac{1}{\alpha^{(\gamma)}\omega^{(\gamma)} + \beta^{(\gamma)}}, \quad \omega^{(\gamma)} = \begin{cases} \frac{2}{M(M+1)} & \text{if } \gamma = a, b \\ \frac{2}{N(N+1)} & \text{if } \gamma = c, d \end{cases}. \tag{15}$$

ensuring $\boldsymbol{A}^{(\gamma)}$ being semi-negative definite. Therefore, the scheme is stable.

## 2.4. Fully-discrete scheme

Equations (7) and (12) are the semi-discrete schemes for one-dimensional and two dimensional space problems, respectively. To march the solution in time, we adopt the Crank-Nicolson (CN) algorithm [4, 17]. We will first present the fully-discrete version of Eq. (7) and then present the fully-discrete version of Eq. (12).

Denote the time step by $\Delta t$ and the discrete time $t_n = n\Delta t$. Let $v_i^n = v_i(t_n) = v(x_i, t_n)$. For convenience we use the notation $v(t_{n+1/2}) = v^{n+1/2} = (v^{n+1} + v^n)/2$, and likewise for other variables. We have the fully-discrete version of Eq. (7), based on the CN method, as

$$\frac{v_j^{n+1} - v_j^n}{\nu\Delta t} = \frac{\partial F(x_i, t_{n+1/2})}{\partial x}, \qquad i = 0, 1, ..., N, \tag{16a}$$

$$v_i^0 = f(x_i), \qquad i = 0, 1, ..., N, \tag{16b}$$

where $F(x, t)$ is given Eq. (7c).

The stability condition obtained at the semi-discrete remains valid for the fully-discrete scheme. Assuming homogeneous boundary conditions, multiplying Eq. (16a) by $2v_i^{n+1/2}\omega_i$,

summing the resultant equations, and following a similar approach shown in the semi-discrete stability analysis, one obtains the following

$$\frac{1}{\nu\Delta t}\sum_{i=0}^{N}\left((v_i^{n+1})^2-(v_i^n)^2\right)\omega_i=(\boldsymbol{V}_-)^T\boldsymbol{A}_-\boldsymbol{V}_-+\boldsymbol{V}_+^T\boldsymbol{A}_+\boldsymbol{V}_+-2\sum_{i=1}^{N-1}\left(\frac{\partial v_i^{n+\frac{1}{2}}}{\partial x}\right)^2\omega_i,$$

where $\boldsymbol{V}_\pm$ and $\boldsymbol{A}_\pm$ given in Eq. (10) with symbols $v_0$ and $v_N$ replaced by $v_0^{n+1/2}$ and $v_N^{n+1/2}$. For $\tau_-$ and $\tau_+$ given by Eq. (11), $\boldsymbol{A}_\pm$ are semi-negative definite. Hence, we have

$$\sum_{i=0}^{N}(v_i^{n+1})^2\omega_i\le\sum_{i=0}^{N}(v_i^n)^2\omega_i\le\cdots\le\sum_{i=0}^{N}f^2(x_i)\omega_i$$

indicating the stability of the fully-discrete scheme.

For computations it is convenient to express the fully-discrete scheme in a matrix-vector representation. We introduce the following notations

$$\boldsymbol{v}^n=[v_0(t_n),v_1(t_n),...,v_N(t_n)]^T,\quad \boldsymbol{I}_i^{(N)}=\mathrm{diag}(\delta_{0i},0,...,\delta_{Ni}),\quad \boldsymbol{e}_i^{(N)}=[\delta_{0i},0,...,\delta_{Ni}]^T,$$

with $\delta_{ij}$ being the Kronecker delta function. Then the fully-discrete scheme can be expressed as

$$\frac{\boldsymbol{v}^{n+1}-\boldsymbol{v}^n}{\nu\Delta t}=\boldsymbol{L}\left(\frac{\boldsymbol{v}^{n+1}+\boldsymbol{v}^n}{2}\right)+\frac{\boldsymbol{g}^{n+1}+\boldsymbol{g}^n}{2},$$
$$\boldsymbol{v}^0=\boldsymbol{f},$$

where $\boldsymbol{f}$ is a vector with $f(x_i)$ being the vector components, $\boldsymbol{L}$ is a matrix operator given as

$$\boldsymbol{L}=\boldsymbol{D}\left(\boldsymbol{D}+\tau_-(\alpha_-\boldsymbol{I}_0^{(N)}-\beta_-\boldsymbol{I}_0^{(N)}\boldsymbol{D})-\tau_+(\alpha_+\boldsymbol{I}_N^{(N)}+\beta_+\boldsymbol{I}_N^{(N)}\boldsymbol{D})\right),$$

with $\boldsymbol{D}$ being the LGL pseudospactral differentiation matrix, and

$$\boldsymbol{g}^m=-\tau_-g_-(t_m)\boldsymbol{D}\boldsymbol{e}_0^{(N)}+\tau_+g_+(t_m)\boldsymbol{D}\boldsymbol{e}_N^{(N)},\quad m=n,n+1.$$

This leads to

$$\left(\boldsymbol{I}-\frac{\nu\Delta t}{2}\boldsymbol{L}\right)\boldsymbol{v}^{n+1}=\left(\boldsymbol{I}+\frac{\nu\Delta t}{2}\boldsymbol{L}\right)\boldsymbol{v}^n+(\nu\Delta t)\left(\frac{\boldsymbol{g}^{n+1}+\boldsymbol{g}^n}{2}\right),$$

with $\boldsymbol{I}$ being the identity matrix. Assuming that $\boldsymbol{I}-\frac{\nu\Delta t}{2}\boldsymbol{L}$ is invertible, we can solve $\boldsymbol{v}^n$ iteratively by providing $\boldsymbol{v}^0$.

Similarly, the fully-discrete scheme for the two-dimensional heat equation, Eq. (12), based on the CN method can be written as

$$\frac{v_{ij}^{n+1}-v_{ij}^{n}}{\nu\Delta t}=\frac{\partial F_x(x_i,y_j,t_{n+1/2})}{\partial x}+\frac{\partial F_y(x_i,y_j,t_{n+1/2})}{\partial y},\quad 0\le i\le M,\,0\le j\le N, \tag{17a}$$

$$v_{ij}(0)=f(x_i,y_j),\qquad 0\le i\le M,\,0\le j\le N, \tag{17b}$$

where $F_x(x,y,t)$ and $F_y(x,y,t)$ are given in Eqs. (12c) and (12d).

The stability condition obtained at the semi-discrete level applicable to the fully-discrete scheme. We can use the same approach to conduct a stability analysis. Assuming homogeneous boundary conditions, multiplying Eq. (17a) by $2v_{ij}^{n+1/2}\omega_{ij}$, summing the resultant equations, and following a similar approach shown in the semi-discrete stability analysis, one obtains the following

$$\frac{1}{\nu\Delta t}\sum_{ij}^{MN}\left((v_{ij}^{n+1})^2-(v_{ij}^{n})^2\right)\omega_{ij}\le\sum_{j=0}^{N}\omega_j^y(\boldsymbol{V}^{(a)})_j^T\boldsymbol{A}^{(a)}\boldsymbol{V}_j^{(a)}+\sum_{j=0}^{N}\omega_j^y(\boldsymbol{V}^{(b)})_j^T\boldsymbol{A}^{(b)}\boldsymbol{V}_j^{(b)}$$
$$+\sum_{i=0}^{M}\omega_i^x(\boldsymbol{V}^{(c)})_i^T\boldsymbol{A}^{(c)}\boldsymbol{V}_i^{(c)}+\sum_{i=0}^{M}\omega_i^x(\boldsymbol{V}^{(d)})_i^T\boldsymbol{A}^{(d)}\boldsymbol{V}_i^{(d)},$$

where $\boldsymbol{V}_j^{(a)}$, $\boldsymbol{V}_j^{(b)}$, $\boldsymbol{V}_i^{(c)}$, $\boldsymbol{V}_i^{(d)}$ and $\boldsymbol{A}^{(\gamma)}$ are given in Eq. (14) with symbols $v_{0j}$, $v_{Mj}$, $v_{i0}$ and $v_{iN}$ replaced by $v_{0j}^{n+1/2}$, $v_{Mj}^{n+1/2}$, $v_{i0}^{n+1/2}$ and $v_{iN}^{n+1/2}$. For $\tau^{(\gamma)}$ given by Eq. (15), $\boldsymbol{A}^{(\gamma)}$ are semi-negative definite. Hence, we can ensure that the fully-discrete scheme is stable.

The fully-discrete scheme also can be written in a matrix-vector form. We define the numerical solution matrix $\boldsymbol{v}^m\in\mathbb{R}^{(M+1)\times(N+1)}$ whose entries are

$$v_{ij}(t_m),\quad 0\le i\le M,\quad 0\le j\le N,\quad m=n,n+1.$$

Thus, the Eq. (17) can be rewritten as

$$\frac{\boldsymbol{v}^{n+1}-\boldsymbol{v}^{n}}{\nu\Delta t}=\boldsymbol{L}\left(\frac{\boldsymbol{v}^{n+1}+\boldsymbol{v}^{n}}{2}\right)+\left(\frac{\boldsymbol{v}^{n+1}+\boldsymbol{v}^{n}}{2}\right)\boldsymbol{R}+\frac{\boldsymbol{g}^{n+1}+\boldsymbol{g}^{n}}{2}+\frac{\boldsymbol{h}^{n+1}+\boldsymbol{h}^{n}}{2}, \tag{18a}$$

$$\boldsymbol{v}^0=\boldsymbol{f}, \tag{18b}$$

where $\boldsymbol{f}\in\mathbb{R}^{(M+1)\times(N+1)}$ with components $f_{ij}=f(x_i,y_j)$, $\boldsymbol{L}$ and $\boldsymbol{R}$ are square matrices operator given as

$$\boldsymbol{L}=\boldsymbol{D}_x(\boldsymbol{D}_x+\tau^{(a)}(\alpha^{(a)}\boldsymbol{I}_0^{(M)}-\beta^{(a)}\boldsymbol{I}_0^{(M)}\boldsymbol{D}_x)-\tau^{(b)}(\alpha^{(b)}\boldsymbol{I}_M^{(M)}+\beta^{(b)}\boldsymbol{I}_M^{(M)}\boldsymbol{D}_x)),$$
$$\boldsymbol{R}=(\boldsymbol{D}_y^T+\tau^{(c)}(\alpha^{(c)}\boldsymbol{I}_0^{(N)}-\beta^{(c)}\boldsymbol{D}_y^T\boldsymbol{I}_0^{(N)})-\tau^{(d)}(\alpha^{(d)}\boldsymbol{I}_N^{(N)}+\beta^{(d)}\boldsymbol{D}_y^T\boldsymbol{I}_N^{(N)}))\boldsymbol{D}_y^T,$$

in which $\boldsymbol{D}_x \in \mathbb{R}^{(M+1)\times(M+1)}$, and $\boldsymbol{D}_y \in \mathbb{R}^{(N+1)\times(N+1)}$ are the LGL pseudospactral differentiation matrices in $x$ and $y$ directions, respectively, and

$$\begin{aligned}
\boldsymbol{g}^m =& -\tau^{(a)} g_-(t_m)\boldsymbol{D}_x \boldsymbol{e}_0^{(M)}(\boldsymbol{e}_0^{(N)})^T + \tau^{(b)} g_+(t_m)\boldsymbol{D}_x \boldsymbol{e}_M^{(M)}(\boldsymbol{e}_N^{(N)})^T, \qquad m = n, n+1,\\
\boldsymbol{h}^m =& \tau^{(c)} h_-(t_m)\boldsymbol{e}_0^{(M)}(\boldsymbol{e}_0^{(N)})^T \boldsymbol{D}_y^T - \tau^{(d)} h_+(t_m)\boldsymbol{e}_M^{(M)}(\boldsymbol{e}_N^{(N)})^T \boldsymbol{D}_y^T, \qquad m = n, n+1.
\end{aligned}$$

Using the above notions, we can rewrite Eq. (18a) as

$$\boldsymbol{\mathcal{A}}\boldsymbol{v}^{n+1} + \boldsymbol{v}^{n+1}\boldsymbol{\mathcal{B}} = \boldsymbol{\mathcal{F}}, \tag{19}$$

where

$$\begin{aligned}
\boldsymbol{\mathcal{A}} =& \frac{1}{2}\boldsymbol{I}^{(M)} - \frac{\nu\Delta t}{2}\boldsymbol{L}, \quad \boldsymbol{\mathcal{B}} = \frac{1}{2}\boldsymbol{I}^{(N)} - \frac{\nu\Delta t}{2}\boldsymbol{R},\\
\boldsymbol{\mathcal{F}} =& \boldsymbol{v}^n + \mathcal{A}\boldsymbol{v}^n + \boldsymbol{v}^n\boldsymbol{\mathcal{B}} + \frac{\nu\Delta t}{2}(\boldsymbol{g}^{n+1} + \boldsymbol{g}^n) + \frac{\nu\Delta t}{2}(\boldsymbol{h}^{n+1} + \boldsymbol{h}^n),
\end{aligned}$$

with $\boldsymbol{I}^{(M)} \in \mathbb{R}^{(M+1)\times(M+1)}$, and $\boldsymbol{I}^{(N)} \in \mathbb{R}^{(N+1)\times(N+1)}$ are identity matrices. Assuming that both $\boldsymbol{\mathcal{A}}$ and $\boldsymbol{\mathcal{B}}$ are diagonalizable, we can solve $\boldsymbol{v}^{n+1}$ by the two-step direct solver [3, 10]. The method is summarized as follows.

## 2.5. Direct solver

Let $\lambda$ and $\varepsilon$ are the eigenvalues of $\boldsymbol{\mathcal{A}}$ and $\boldsymbol{\mathcal{B}}$, respectively. $\boldsymbol{P}$ and $\boldsymbol{Q}$ are associated eigenvector matrices, that is,

$$\boldsymbol{P}^{-1}\boldsymbol{\mathcal{A}} = \boldsymbol{\Lambda}_{\mathcal{A}}\boldsymbol{P}^{-1}, \quad \boldsymbol{\mathcal{B}}\boldsymbol{Q} = \boldsymbol{Q}\boldsymbol{\Lambda}_{\mathcal{B}}, \tag{21}$$

where $\boldsymbol{\Lambda}_{\mathcal{A}} = \mathrm{diag}(\lambda_1, \cdots, \lambda_{M+1})$, and $\boldsymbol{\Lambda}_{\mathcal{B}} = \mathrm{diag}(\varepsilon_1, \cdots, \varepsilon_{N+1})$. Then, multiplying Eq. (19) by $\boldsymbol{P}^{-1}$ from the left, and by $\boldsymbol{Q}$ from the right, and using Eq. (21), we get for s given pair $(i, j)$,

$$\sum_{i'=1}^{M+1}\sum_{j'=1}^{N+1} P_{ii'}^{-1} v_{i'j'}^{n+1} Q_{j'j} = \frac{1}{\lambda_i + \varepsilon_j}\sum_{i'=1}^{M+1}\sum_{j'=1}^{N+1} P_{ii'}^{-1}\mathcal{F}_{i'j'}Q_{j'j}.$$

Define a matrix $\boldsymbol{G}$ with entries given as

$$G_{ij} = \frac{1}{\lambda_i + \varepsilon_j}\sum_{i'=1}^{M+1}\sum_{j'=1}^{N+1} P_{ii'}^{-1}\mathcal{F}_{i'j'}Q_{j'j}.$$

We can get solution matrix $\boldsymbol{v}^{n+1}$ as

$$\boldsymbol{v}^{n+1} = \boldsymbol{P}\boldsymbol{G}\boldsymbol{Q}^{-1}.$$

# 3. Numerical Result

In this study, we provide convergence study results illustrating the performance of the methods.

Through out the whole report, we compute time step $\Delta t$ as

$$\Delta t = \frac{\text{CFL}}{\nu \text{D} N}$$

unless stated otherwise, where CFL is the Courant-Friedrichs-Lewy number, and D is the number of the space dimension. To measure the performance of the scheme, we measure the maximum pointiest error $\epsilon(N)$ and the order of convergence $q$ defined as

$$\|\epsilon(N)\|_\infty = \max_{ij} |u_{ij} - v_{ij}|, \quad q = \frac{\log \frac{\|\epsilon(N_1)\|_\infty}{\|\epsilon(N_2)\|_\infty}}{\log \frac{N_2}{N_1}}, \tag{22}$$

where $N$, $N_1$ and $N_2$ are the degrees of the approximation solutions, and where $u_{ij}$ and $v_{ij}$ are the pointiest exact and numerical solutions, respectively.

## 3.1. One-dimensional problem

Consider the one-dimensional heat equation

$$\frac{\partial u(x,t)}{\partial t} = \frac{\partial^2 u(x,t)}{\partial x^2}, \qquad x \in \mathsf{I}, \quad t \geq 0, \tag{23a}$$

$$u(x,0) = \sin(k\pi x), \qquad x \in \mathsf{I}, \tag{23b}$$

$$\mathcal{B}_\pm u(\pm 1, t) = (\alpha_\pm \sin(\pm k\pi) \pm \beta_\pm k\pi \cos(\pm k\pi)) e^{-k\pi^2 t}, \qquad t > 0. \tag{23c}$$

The exact solution to the problem is given as

$$u(x,t) = e^{-k^2\pi^2 t} \sin(\pi x).$$

We use the one-dimentional scheme, Eq. (16), to solve the problem with boundary conditions imposed at $x = \pm 1$ of different kinds. The penalty parameters are computed by Eq. (11). The convergence study results are illustrated in Table 1-5.

In our computation experiments, we choose $T = 0.1$, and $k = 2$ with six different combinations of boundary conditions at $x = \pm 1$. From these results, we see that the error decreases when the degree of the approximation polynomial $N$ increases. The convergence

Table 1: Maximum error and converge rate of Eq. (23) subject to both Dirichlet boundary conditions ($\alpha_{\pm} = 1, \beta_{\pm} = 0$) at $x = \pm 1$.

| $N$ | CFL = 0.1 | | CFL = 0.25 | | CFL = 0.5 | |
|---|---|---|---|---|---|---|
| | error | order | error | order | error | order |
| 8 | 5.28E-04 | - | 2.48E-03 | - | 8.32E-03 | - |
| 12 | 2.07E-04 | 2.31 | 1.22E-03 | 1.75 | 4.54E-03 | 1.49 |
| 16 | 1.16E-04 | 2.03 | 6.87E-04 | 2.00 | 2.75E-03 | 1.74 |
| 20 | 7.35E-05 | 2.03 | 4.60E-04 | 1.79 | 1.85E-03 | 1.77 |

Table 2: Maximum error and converge rate of Eq. (23) subject to Dirichlet and Neumann boundary conditions ($\alpha_{-} = 1, \alpha_{+} = 0, \beta_{-} = 0, \beta_{+} = 1$) at $x = -1$ and $x = 1$, respectively.

| $N$ | CFL = 0.1 | | CFL = 0.25 | | CFL = 0.5 | |
|---|---|---|---|---|---|---|
| | error | order | error | order | error | order |
| 8 | 9.64E-04 | - | 3.23E-03 | - | 1.05E-02 | - |
| 12 | 2.29E-04 | 3.55 | 1.36E-03 | 2.13 | 5.11E-03 | 1.79 |
| 16 | 1.31E-04 | 1.93 | 7.83E-04 | 1.93 | 3.12E-03 | 1.71 |
| 20 | 8.45E-05 | 1.98 | 5.28E-04 | 1.77 | 2.12E-03 | 1.74 |

Table 3: Maximum error and converge rate of Eq. (23) subject to Dirichlet and Robin boundary conditions ($\alpha_{\pm} = 1, \beta_{-} = 0, \beta_{+} = 1$) at $x = -1$ and $x = 1$, respectively.

| $N$ | CFL = 0.1 | | CFL = 0.25 | | CFL = 0.5 | |
|---|---|---|---|---|---|---|
| | error | order | error | order | error | order |
| 8 | 8.78E-04 | - | 3.09E-03 | - | 1.01E-02 | - |
| 12 | 2.25E-04 | 3.36 | 1.33E-03 | 2.08 | 4.94E-03 | 1.77 |
| 16 | 1.29E-04 | 1.93 | 7.69E-04 | 1.90 | 3.06E-03 | 1.66 |
| 20 | 8.26E-05 | 2.00 | 5.17E-04 | 1.78 | 2.07E-03 | 1.76 |

Table 4: Maximum error and converge rate of Eq. (23) subject to Neumann and Robin boundary conditions ($\alpha_- = 0, \alpha_+ = 1, \beta_\pm = 1$) at $x = -1$ and $x = 1$, respectively.

| $N$ | CFL = 0.1 | | CFL = 0.25 | | CFL = 0.5 | |
|---|---|---|---|---|---|---|
| | error | order | error | order | error | order |
| 8 | 9.64E-04 | - | 3.23E-03 | - | 1.05E-02 | - |
| 12 | 2.29E-04 | 3.55 | 1.36E-03 | 2.13 | 5.10E-03 | 1.79 |
| 16 | 1.31E-04 | 1.93 | 7.83E-04 | 1.93 | 3.12E-03 | 1.71 |
| 20 | 8.45E-05 | 1.98 | 5.28E-04 | 1.77 | 2.12E-03 | 1.74 |

Table 5: Maximum error and converge rate of Eq. (23) subject to Neumann boundary conditions ($\alpha_- = 0, \alpha_+ = 1, \beta_- = 0, \beta_+ = 1$) at $x = \pm 1$.

| $N$ | CFL = 0.1 | | CFL = 0.25 | | CFL = 0.5 | |
|---|---|---|---|---|---|---|
| | error | order | error | order | error | order |
| 8 | 1.96E-03 | - | 5.45E-03 | - | 1.90E-02 | - |
| 12 | 4.38E-04 | 3.69 | 2.60E-03 | 1.82 | 9.75E-03 | 1.65 |
| 16 | 2.38E-04 | 2.12 | 1.43E-03 | 2.09 | 5.69E-03 | 1.87 |
| 20 | 1.58E-04 | 1.84 | 9.90E-04 | 1.64 | 3.98E-03 | 1.61 |

Table 6: Maximum error and converge rate of Eq. (23) subject to both Robin boundary conditions ($\alpha_\pm = 1, \beta_\pm = 1$) at $x = \pm 1$.

| $N$ | CFL = 0.1 | | CFL = 0.25 | | CFL = 0.5 | |
|---|---|---|---|---|---|---|
| | error | order | error | order | error | order |
| 8 | 8.78E-04 | - | 3.09E-03 | - | 1.01E-02 | - |
| 12 | 2.25E-04 | 3.36 | 1.33E-03 | 2.08 | 4.94E-03 | 1.77 |
| 16 | 1.29E-04 | 1.93 | 7.69E-04 | 1.90 | 3.06E-03 | 1.66 |
| 20 | 8.26E-05 | 2.00 | 5.17E-04 | 1.78 | 2.07E-03 | 1.75 |

Table 7: Maximum error and converge rate of Eq. (24). Computational parameters: $\nu = 1$, $k = 2$, $T = 0.1$.

| $N$ | CFL = 0.1 | | CFL = 0.25 | | CFL = 0.5 | |
|---|---|---|---|---|---|---|
| | error | order | error | order | error | order |
| 12 | 9.24E-03 | - | 9.58E-03 | - | 1.01E-02 | - |
| 14 | 5.81E-04 | 17.95 | 5.56E-04 | 18.47 | 8.46E-04 | 16.11 |
| 16 | 3.07E-05 | 22.03 | 1.33E-04 | 10.68 | 5.03E-04 | 3.89 |
| 18 | 1.93E-05 | 3.95 | 1.09E-04 | 1.73 | 3.37E-04 | 3.40 |

rate is second order accurate. While the CFL increases, the error also increases because the time step increases, for the same $N$.

In the previous example, the solution vanishes as time evolves. Consequently, we are unable to know whether the scheme is stable after long-time computations. Hence, we consider the following problem which has an exact solution profile that does not vanish as time evolves. Consider the problem:

$$\frac{\partial u(x,t)}{\partial t} = \nu \frac{\partial^2 u(x,t)}{\partial x^2} + F(x,t), \qquad x \in \mathsf{I}, t > 0, \tag{24a}$$

$$u(x,0) = \sin(k\pi x), \qquad x \in \mathsf{I}, \tag{24b}$$

$$\mathcal{B}_{\pm} u(\pm 1, t) = \sin(k\pi(\pm 1 - t)) \pm \pi \cos(k\pi(\pm 1 - t)), \qquad t > 0, \tag{24c}$$

where $F(x,t)$ is a source term given explicitly

$$F(x,t) = \nu k^2 \pi^2 \sin(k\pi(x-t)) - k\pi \cos(k\pi(x-t)).$$

The solution of the problem is

$$u(x,t) = \sin(k\pi(x-t)).$$

In the following computations, we use different combinations of $\nu$, $k$, and $T$. The convergence results are shown in Table 7-10. The exact and numerical solution at time $T = 0.1$ are plot at Figure 1 for different values of $N$. The exact and numerical solution from $T = 0$ to $T = 1$ with $N = 16$ are plot at Figure 2.

Table 8: Maximum error and converge rate of Eq. (24). Computational parameters: $\nu = 2$, $k = 2$, $T = 0.1$.

| $N$ | CFL = 0.1 | | CFL = 0.25 | | CFL = 0.5 | |
|---|---|---|---|---|---|---|
| | error | order | error | order | error | order |
| 12 | 1.60E-02 | - | 1.59E-02 | - | 1.68E-02 | - |
| 14 | 1.01E-03 | 17.89 | 1.00E-03 | 17.93 | 9.32E-04 | 18.76 |
| 16 | 4.81E-05 | 22.83 | 5.34E-05 | 21.97 | 8.08E-05 | 18.31 |
| 18 | 4.11E-06 | 20.88 | 1.65E-05 | 9.97 | 6.08E-05 | 2.41 |

Table 9: Maximum error and converge rate of Eq. (24). Computational parameters: $\nu = 2$, $k = 3$, $T = 0.1$.

| $N$ | CFL = 0.1 | | CFL = 0.25 | | CFL = 0.5 | |
|---|---|---|---|---|---|---|
| | error | order | error | order | error | order |
| 16 | 4.41E-02 | - | 4.43E-02 | - | 4.46E-02 | - |
| 18 | 3.90E-03 | 20.58 | 3.95E-03 | 20.52 | 3.96E-03 | 20.56 |
| 20 | 2.64E-04 | 25.55 | 2.88E-04 | 24.84 | 3.96E-04 | 21.86 |
| 22 | 1.80E-05 | 28.22 | 3.50E-05 | 22.12 | 1.02E-04 | 14.20 |

Table 10: Maximum error and converge rate of Eq. (24). Computational parameters: $\nu = 1$, $k = 2$, CFL= 0.25.

| $N$ | T = 0.1 | | T = 1 | | T = 10 | | T = 100 | |
|---|---|---|---|---|---|---|---|---|
| | error | order | error | order | error | order | error | order |
| 12 | 9.58E-3 | - | 2.45E-3 | - | 2.44E-3 | - | 2.44E-03 | - |
| 14 | 5.56E-4 | 18.47 | 4.93E-4 | 10.39 | 4.95E-4 | 10.35 | 4.95E-04 | 10.35 |
| 16 | 1.33E-4 | 10.68 | 2.72E-4 | 4.46 | 2.73E-4 | 4.45 | 2.73E-04 | 4.45 |
| 18 | 1.09E-4 | 1.73 | 2.12E-4 | 2.10 | 2.13E-4 | 2.10 | 2.13E-04 | 2.10 |

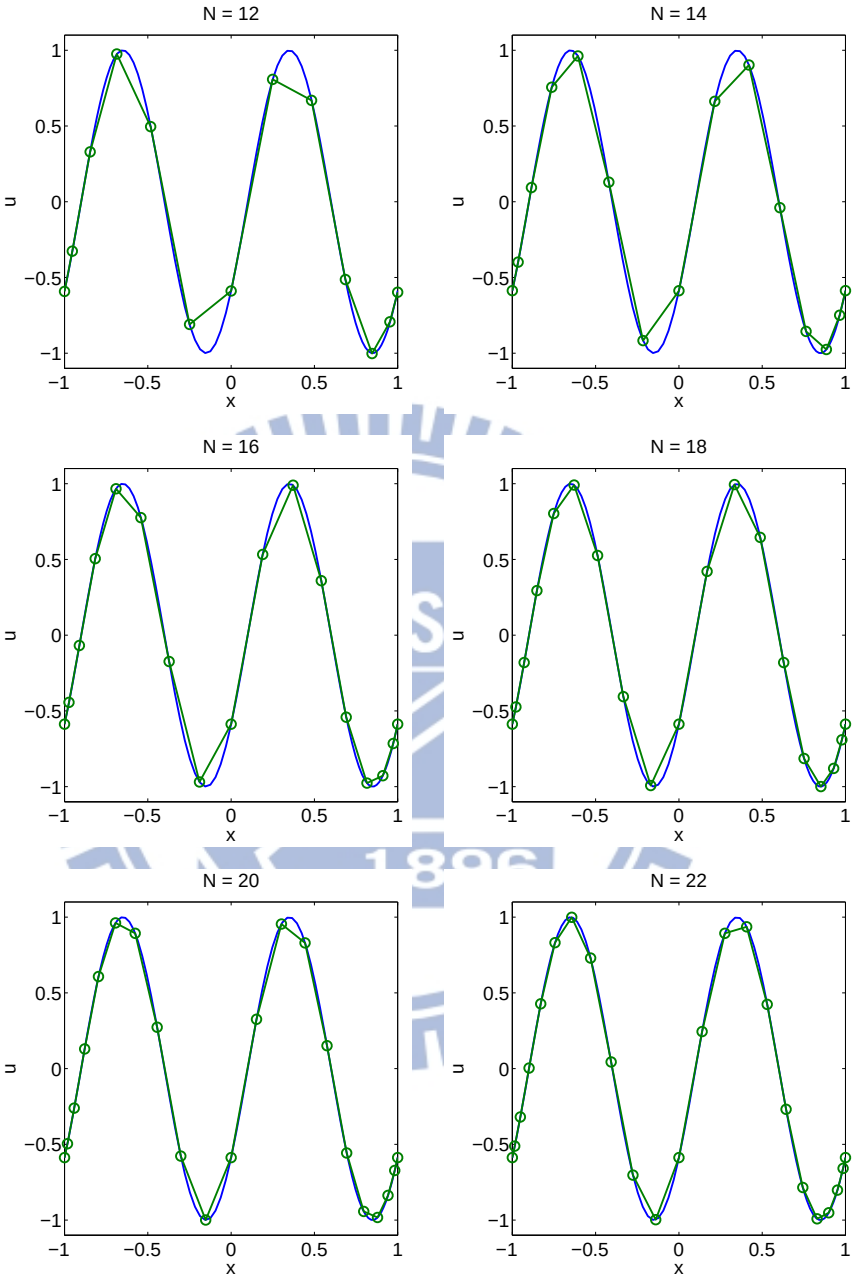


Figure 1: Numerical solution profiles (green lines with hallow circle markers) obtained by Eq. (24) for various values of $N$ at $T = 0.1$, and the corresponding exact solution profiles (solid blue lines). Computational parameters: $\nu = 1$, $k = 2$.

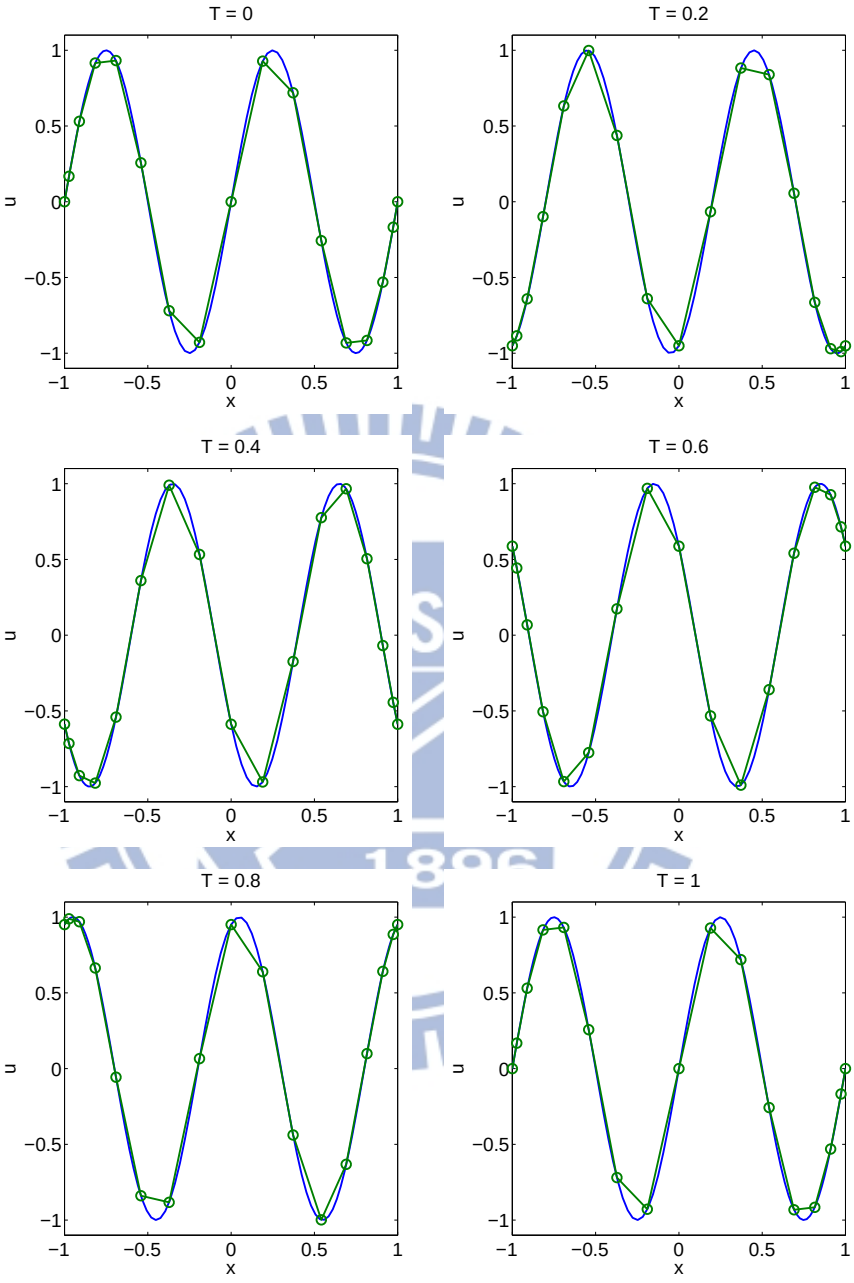


Figure 2: Field plots of the numerical solution profiles (green lines with hallow circle markers) obtained by Eq. (24) at different times, and the exact solution profiles (solid blue lines) at the corresponding time. Computational parameters: $\nu = 1$, $k = 2$, CFL$= 0.25$.

Table 11: Maximum error and converge rate of Eq. (24) subject to $h\Delta t = \mathrm{CFL}/(\nu N^2)$. The boundary conditions and computational parameters are given in Table 7.

| $N$ | CFL = 0.1 | | CFL = 0.25 | | CFL = 0.5 | |
|---|---|---|---|---|---|---|
| | error | order | error | order | error | order |
| 12 | 9.25E-03 | - | 9.25E-03 | - | 9.25E-03 | - |
| 14 | 5.78E-04 | 8.99 | 5.78E-04 | 8.99 | 5.78E-04 | 8.99 |
| 16 | 2.66E-05 | 11.53 | 2.66E-05 | 11.53 | 2.64E-05 | 11.56 |
| 18 | 9.49E-07 | 14.15 | 9.79E-07 | 14.01 | 2.03E-06 | 10.89 |

From Table 7-10, the error decreases when $N$ increases, and the convergence rate is second order accuracy. For same total number of grid points, the error increases when the CFL increases. When we increase the number of $k$, we need to use more grid points to achieve second-order convergence result. In this example, we can extend the terminal time $T$ to 100, and the numerical result still have second-order convergence. Figure 1 shows that our scheme captures the behavior of wave with few grid points. Figure 2 shows that if we extend the computational time $T$, the waveform does not change when $T$ extends.

In the previous experiments the computational time step $\Delta t$ are of $\mathcal{O}(1/N)$, and the convergence second order accurate, which clearly demonstrated the convergence rate of the CN method. To illustrate the exponential convergence of the scheme due to the spectral method, we use the same equation, Eq. (24) and the same computational parameters given in Table 7, but with time step $\Delta t$, and the convergence order $q$ computed as

$$\Delta t = \frac{\mathrm{CFL}}{\nu \mathrm{D} N^2}, \quad q = \frac{\log \frac{\|\epsilon(N_1)\|_\infty}{\|\epsilon(N_2)\|_\infty}}{2 \log \frac{N_2}{N_1}}.$$

Notice that the time step is smaller than that in the pervious experiments. The numerical results are shown in Table 11.

Indeed, comparing the results shown in Table 7 and Table 11, we observe exponential convergence of the numerical results as the degree of the approximation solution $N$ increases. However, due to the smaller time step the numerical experiments require more computational time to conduct.

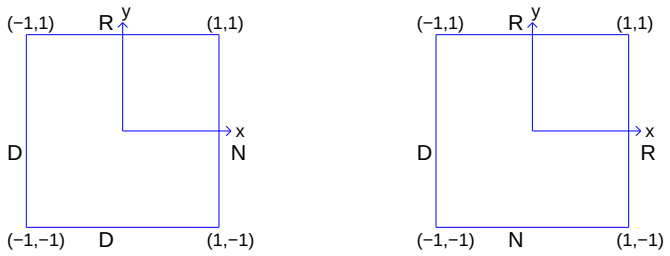


(a) (b)

Figure 3: Description of the boundary conditions enforced at the four edges of the square domain $[-1,1]^2$. The letters N, D, and R are designated as the Neumann, Dirichlet, and Robin boundary conditions, respectively. The values of the associated parameters $\alpha$ and $\beta$ on each edge are: $(\alpha,\beta)=(1,0)$ if Dirichlet boundary condition is applied; $(\alpha,\beta)=(0,1)$ if Neumann boundary condition is applied; $(\alpha,\beta)=(1,1)$ if Robin boundary condition is applied.

## 3.2. Two-dimensional problem

We now present convergence results of the methods for two dimensional examples. Consider

$$u(x,y,t)=e^{-k^2\pi^2 t}\sin(k\pi x)\sin(k\pi y)$$

satisfying the following two-dimensional heat equation

$$\frac{\partial u}{\partial t}=\frac{\partial^2 u}{\partial x^2}+\frac{\partial^2 u}{\partial y^2},\quad \boldsymbol{x}\in \mathsf{I}^2,\quad t\geq 0, \tag{25a}$$

$$u(x,y,0)=\sin(k\pi x)\sin(k\pi y),\quad \boldsymbol{x}\in \mathsf{I}^2, \tag{25b}$$

$$\mathcal{B}^{(a)}u(-1,y,t)=\left(\alpha^{(a)}\sin(-k\pi)-\beta^{(a)}k\pi\cos(-k\pi)\right)e^{-k^2\pi^2 t}\sin(k\pi y),\quad t\geq 0, \tag{25c}$$

$$\mathcal{B}^{(b)}u(+1,y,t)=\left(\alpha^{(b)}\sin(+k\pi)+\beta^{(b)}k\pi\cos(+k\pi)\right)e^{-k^2\pi^2 t}\sin(k\pi y),\quad t\geq 0, \tag{25d}$$

$$\mathcal{B}^{(c)}u(x,-1,t)=\left(\alpha^{(c)}\sin(-k\pi)-\beta^{(c)}k\pi\cos(-k\pi)\right)e^{-k^2\pi^2 t}\sin(k\pi x),\quad t\geq 0, \tag{25e}$$

$$\mathcal{B}^{(d)}u(x,+1,t)=\left(\alpha^{(d)}\sin(+k\pi)+\beta^{(d)}k\pi\cos(+k\pi)\right)e^{-k^2\pi^2 t}\sin(k\pi x),\quad t\geq 0. \tag{25f}$$

In this example, the boundary conditions on the four edges are illustrated in Figure (3) with parameters chosen as $T=0.5$, $k=2$. The convergence study results are presented in Table 12 and 13.

From the results shown in Table 12 and 13, the numerical result as we expected. In this example, the solution vanishes to 0 when we extend the terminal time $T$. Hence,

Table 12: Maximum error and converge rate of Eq. (25) subject to boundary conditions specified in Figure 3(a). Computational parameters: $k = 2$, $T = 0.5$.

| $N$ | CFL = 0.1 | | CFL = 0.25 | | CFL = 0.5 | |
|---|---|---|---|---|---|---|
| | error | order | error | order | error | order |
| $12 \times 12$ | 6.86E-05 | - | 4.25E-04 | - | 1.66E-03 | - |
| $14 \times 14$ | 5.05E-05 | 1.98 | 3.14E-04 | 1.97 | 1.24E-03 | 1.88 |
| $16 \times 16$ | 3.88E-05 | 1.98 | 2.41E-04 | 1.97 | 9.54E-04 | 1.96 |
| $18 \times 18$ | 3.05E-05 | 2.03 | 1.90E-04 | 2.02 | 7.59E-04 | 1.94 |

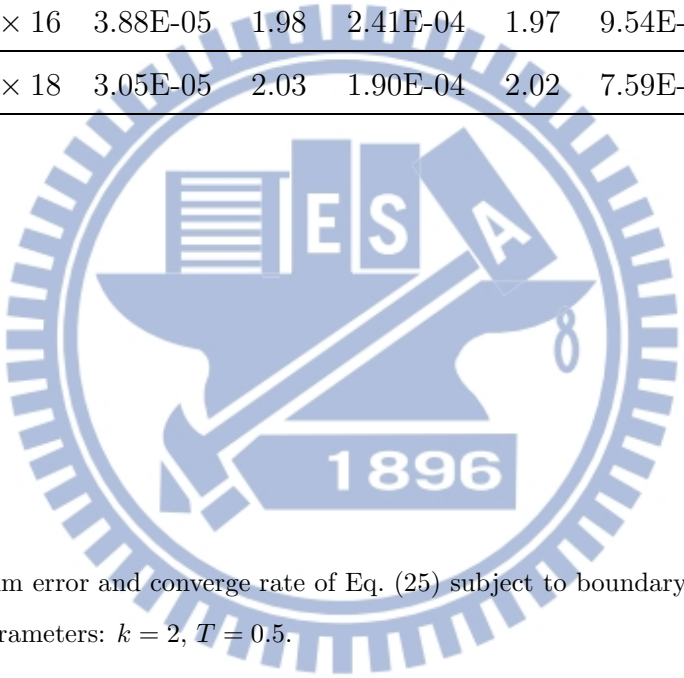

Table 13: Maximum error and converge rate of Eq. (25) subject to boundary conditions in Figure 3(b). Computational parameters: $k = 2$, $T = 0.5$.

| $N$ | CFL = 0.1 | | CFL = 0.25 | | CFL = 0.5 | |
|---|---|---|---|---|---|---|
| | error | order | error | order | error | order |
| $12 \times 12$ | 5.75E-05 | - | 3.57E-04 | - | 1.39E-03 | - |
| $14 \times 14$ | 4.24E-05 | 1.98 | 2.63E-04 | 1.97 | 1.04E-03 | 1.88 |
| $16 \times 16$ | 3.25E-05 | 1.98 | 2.02E-04 | 1.97 | 8.01E-04 | 1.96 |
| $18 \times 18$ | 2.56E-05 | 2.03 | 1.59E-04 | 2.02 | 6.38E-04 | 1.93 |

we can not observe the stability of the scheme after a long time computations. We also design a two-dimensional example involving inhomogeneous source term as follows.

Consider the problem with inhomogeneous source term

$$\frac{\partial u}{\partial t} = \frac{\partial^2 u}{\partial x^2} + \frac{\partial^2 u}{\partial y^2} + F(x,y,t), \quad \boldsymbol{x} \in \mathsf{I}^2, \quad t \geq 0 \tag{26a}$$

$$u(x,y,0) = \sin(\pi x)\sin(\pi y), \quad \boldsymbol{x} \in \mathsf{I}^2, \quad t \geq 0, \tag{26b}$$

$$\begin{aligned}\mathcal{B}^{(a)}u(-1,y,t) =& \alpha^{(a)}\sin(k\pi(-1-t))\sin(k\pi y) \\ & - \beta^{(a)}k\pi\cos(k\pi(-1-t))\sin(k\pi y), \quad t \geq 0,\end{aligned} \tag{26c}$$

$$\begin{aligned}\mathcal{B}^{(b)}u(+1,y,t) =& \alpha^{(b)}\sin(k\pi(+1-t))\sin(k\pi y) \\ & + \beta^{(b)}k\pi\cos(k\pi(+1-t))\sin(k\pi y), \quad t \geq 0,\end{aligned} \tag{26d}$$

$$\mathcal{B}^{(c)}u(x,-1,t) = \big(\alpha^{(c)}\sin(-k\pi) - \beta^{(c)}k\pi\cos(-k\pi)\big)\sin(k\pi x - k\pi t), \quad t \geq 0, \tag{26e}$$

$$\mathcal{B}^{(d)}u(x,+1,t) = \big(\alpha^{(d)}\sin(+k\pi) + \beta^{(d)}k\pi\cos(+k\pi)\big)\sin(k\pi x - k\pi t), \quad t \geq 0, \tag{26f}$$

where $F(x,y,t)$ is a source term given explicitly as

$$F(x,y,t) = -k\pi\cos(k\pi(x-t))\sin(k\pi y) + 2(k\pi)^2\sin(k\pi(x-t))\sin(k\pi y).$$

The exact solution to the problem is

$$u(x,y,t) = \sin(k\pi(x-t))\sin(k\pi y).$$

For numerical experiments, the boundary conditions are specified in Figure 4, and the parameters are given as $k = 2$, $T = 0.5$, CFL$= 0.25$. The numerical result on presented in Table 14 and Table 15. Table 16 presents the numerical results with boundary conditions in specified in Figure 4(d), and the parameters are given as $k = 2$, CFL$= 0.25$.

From these experiments, we observe that the error decreases when $N$ increases, and the convergence rate is of second-order accuracy. When we extend the terminal time $T$ to 100, we still have second-order convergence.

# 4. Concluding remarks

In this study, we proposed a stable pseudospectral penalty scheme for heat equations. The scheme is based on Legendre psudospectral penalty method in space and Crank-Nicolson

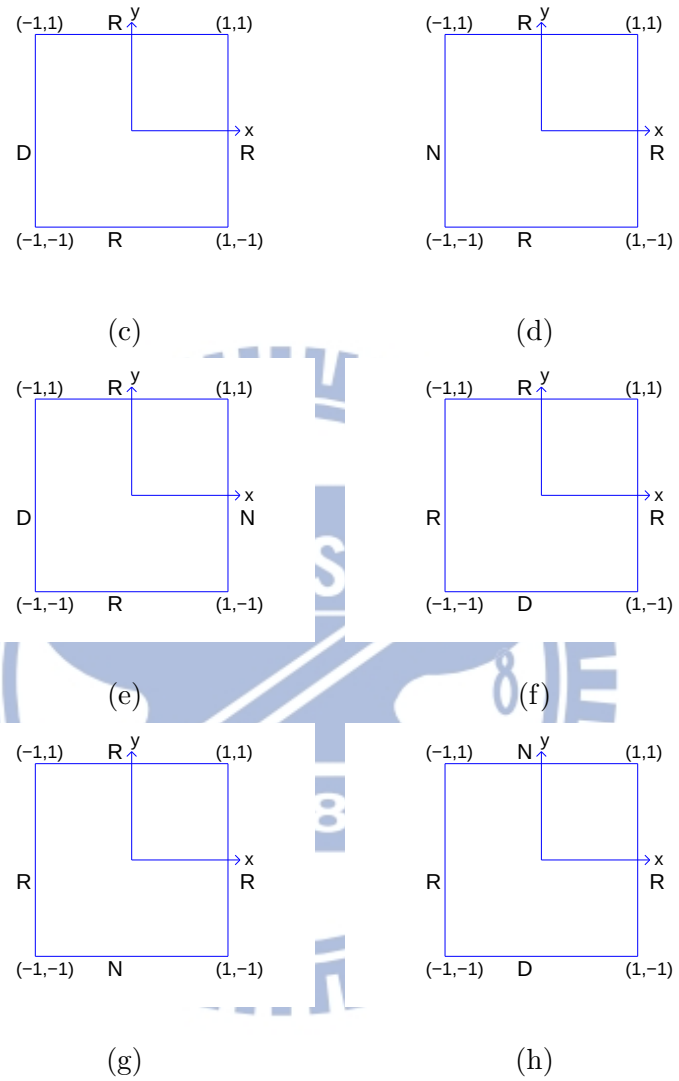


Figure 4: Description of the boundary conditions enforced at the four edges of the square domain $[-1,1]^2$. The letters N, D, and R are designated as the Neumann, Dirichlet, and Robin boundary conditions, respectively. The values of the associated parameters $\alpha$ and $\beta$ on each edge are: $(\alpha,\beta)=(1,0)$ if Dirichlet boundary condition is applied; $(\alpha,\beta)=(0,1)$ if Neumann boundary condition is applied; $(\alpha,\beta)=(1,1)$ if Robin boundary condition is applied.

Table 14: Maximum error and converge rate of Eq. (26) subject to boundary conditions given in Figure (4). Computational parameters: $T = 0.5$, $k = 2$, CFL= 0.25.

| $N \times N$ | Fig. (c) | | Fig. (d) | | Fig. (e) | |
|---|---|---|---|---|---|---|
| | error | order | error | order | error | order |
| $12 \times 12$ | 1.10E-02 | - | 1.13E-02 | - | 1.07E-02 | - |
| $14 \times 14$ | 6.71E-04 | 18.13 | 6.94E-04 | 18.12 | 6.85E-04 | 17.83 |
| $16 \times 16$ | 4.56E-05 | 20.14 | 4.71E-05 | 20.15 | 5.47E-05 | 18.93 |
| $18 \times 18$ | 1.91E-05 | 7.39 | 1.93E-05 | 7.57 | 2.57E-05 | 6.40 |
| $20 \times 20$ | 1.57E-05 | 1.85 | 1.56E-05 | 2.00 | 2.11E-05 | 1.89 |

Table 15: Maximum error and converge rate of Eq. (26) subject to boundary conditions given in Figure (4). Computational parameters: $T = 0.5$, $k = 2$, CFL= 0.25.

| $N \times N$ | Fig. (f) | | Fig. (g) | | Fig. (h) | |
|---|---|---|---|---|---|---|
| | error | order | error | order | error | order |
| $12 \times 12$ | 1.13E-02 | - | 1.67E-02 | - | 1.72E-02 | - |
| $14 \times 14$ | 6.94E-04 | 18.12 | 1.07E-03 | 17.85 | 1.10E-03 | 17.85 |
| $16 \times 16$ | 4.71E-05 | 20.15 | 7.07E-05 | 20.33 | 7.22E-05 | 20.37 |
| $18 \times 18$ | 1.93E-05 | 7.57 | 2.26E-05 | 9.70 | 2.27E-05 | 9.81 |
| $20 \times 20$ | 1.56E-05 | 2.00 | 1.78E-05 | 2.22 | 1.80E-05 | 2.22 |

Table 16: Maximum error and converge rate of Eq. (26) subject to boundary conditions given as N-R in x axis, and R-R in y axis. Computational parameters: $k = 2$, CFL= 0.25.

| $N \times N$ | T=0.1 | | T=1 | | T=10 | | T=100 | |
|---|---|---|---|---|---|---|---|---|
| | error | order | error | order | error | order | error | order |
| $12 \times 12$ | 2.43E-05 | - | 2.68E-05 | - | 2.99E-05 | - | 1.01E-02 | - |
| $14 \times 14$ | 1.48E-05 | 3.21 | 1.82E-05 | 2.52 | 1.92E-05 | 2.88 | 6.17E-04 | 18.16 |
| $16 \times 16$ | 1.09E-05 | 2.28 | 1.36E-05 | 2.18 | 1.43E-05 | 2.18 | 4.30E-05 | 19.95 |
| $18 \times 18$ | 8.75E-06 | 1.89 | 1.11E-05 | 1.75 | 1.17E-05 | 1.72 | 1.90E-05 | 6.92 |
| $20 \times 20$ | 7.47E-06 | 1.51 | 8.96E-06 | 1.99 | 9.45E-06 | 2.02 | 1.55E-05 | 1.96 |

method in time. The boundary conditions are enforced through the penalty method. By conducting discrete energy estimates, we determine the values of the penalty parameters which are suitable for the stable computations. A series of numerical results showed that the convergence rate is consistent with the theoretical stability analysis.

In the future, we hope to adopt a high order numerical scheme in time such as using Runge-Kutta method. Furthermore, We hope to develop methods for anisotropic heat equations or Schrödinger equations.

# References


[1] F. Black, M. Scholes, The pricing of options and corporate liabilities. Journal of Political Economy, 81, 3 (1973) 637-654.

[2] J. R. Cannon, The One-Dimensional Heat Equation. Cambridge University Press, Vol. 23, (1984).

[3] H. Chen, Y. Su, B. D. Shizgal, A direct spectral collocation Poisson solver in polar and cylinder coordinates. J. Comput. Phys., 160, 2 (2000) 453-469.

[4] J. Crank, P. Nicolson. A practical method for numerical evaluation of solutions of partial differential equations of the heat conduction type. Proc. Camb. Phil. Soc., 43, 1 (1947) 50-67.

[5] N. Foster, and R. Fedkiw, Practical Animation of Liquids. Computer Graphics SIGGRAPH (2001) 15-22.

[6] D. Funaro, D. Gottlieb, A new method of imposing boundary conditions in pseudospectral approximations of hyperbolic equations. Math. Comput. 51 (1988) 599-613.

[7] J.S. Hesthaven, S. Gottlieb, D. Gottlieb, Spectral Methods for Time-Dependent Problems. Cambridge Universuty Press. Prentice Hall, (2007) .

[8] E. Isaacson, H. Bishop Keller, Analysis of Numerical Methods. Wiley, (1966).

[9] P. D. Lax, R. D. Richtmyer, Survey of the stability of linear finite difference equations. Communications on Pure and Applied Mathematics, 9 (1956) 267-293.

[10] R. E. Lynch, J. R. Rice, and D. H. Thomas, Direct solution of partial different equations by tensor product methods. Numer. Math., 6 (1964) 185-199.

[11] M. Mimura, H. Sakaguchi, M. Matsuchita, Reaction diffusion modelling of bacterial colony patterns. Physica A, 282 (2000) 283-303.

[12] F. de Monte, Transient heat conduction in one-dimensional composite slab. A 'natural' analytic approach. Int. J. Heat Mass Transfer, 43 19 (2000) 3607-3616.

[13] J. von Neumann, Proposal and analysis of a numerical method for the treatment of hydro-dynamical shock problems. Nat. Def. Res.Com., Report AM-551.

[14] B.Perthame, Growth, reaction, movement and diffusion from biology. Lecture Notes, University Paris (2012).

[15] P. Perona, J. Malik, Scale-space and edge detection using anisotropic diffusion. IEEE Trans., 12, 7 (1990) 629-639.

[16] G. W. Recktenwald, Finite-Difference Approximations to the Heat Equation. Class Notes, (2004).

[17] G. D. Smith, Numerical Solution of Partial Differential Equations: Finite Difference Methods. Oxford (1985).

[18] C. H. Teng, M. Min, J. K. Wang, Pseudospectral and Runge-Kutta-Nyström methods for second-order wave equations: Stable and accurate boundary treatments. in submission.

[19] P. Wilmott, S. Howison, J. Dewynne, The Mathematics of Financial Derivatives:A Student Introduction. Cambridge Univ. Press, (1995).

# Appendix

## A. Stability analysis of one-dimensional semi-discrete schemes

Assuming homogeneous boundary conditions, multiplying Eq. (7a) by $\nu^{-1}v_i\omega_i$ and summing over the index $i = 0$ to $N$, we have the energy rate equation of the form

$$\frac{1}{\nu}\sum_{i=0}^{N}\omega_i v_i \frac{\partial v}{\partial t}\Big|_i = \sum_{i=0}^{N}\omega_i v_i \frac{\partial F(x_i,t)}{\partial x}.$$

The left hand side can be written as

$$\frac{1}{\nu}\sum_{i=0}^{N} v_i\omega_i \frac{\partial v}{\partial t}\Big|_i = \frac{1}{2\nu}\frac{d}{dt}\sum_{i=0}^{N} v_i^2\omega_i.$$

There has three term on the right hand side, we will discuss each one as follows, respectively. The first term of right hand side

$$\begin{aligned}\sum_{i=0}^{N}\left(v\omega\frac{\partial^2 v}{\partial x^2}\Big|_i\right) &= \int_{-1}^{1} v d\left(\frac{\partial v}{\partial x}\right) = \left[v\frac{\partial v}{\partial x}\Big|_{-1}^{1} - \int_{-1}^{1}\left(\frac{\partial v}{\partial x}\right)^2 dx\right] \\ &= \left[v_N\frac{\partial v_N}{\partial x} - v_0\frac{\partial v_0}{\partial x} - \sum_{i=0}^{N}\left(\omega_i\frac{\partial v_i}{\partial x}\right)^2\right].\end{aligned}$$

The second term of right hand side

$$\begin{aligned}\sum_{i=0}^{N}\tau_0\ell_0'(x_i)\left(\alpha_- v_0 - \beta_-\frac{\partial v_0}{\partial x}\right)v_i\omega_i &= \alpha_-\tau_0 v_0\int_{-1}^{1} v\ell_0'(x)dx - \beta_-\tau_0\frac{\partial v_0}{\partial x}\int_{-1}^{1} v\ell_0'(x)dx \\ &= \left(\alpha_-\tau_0 v_0 - \beta_-\tau_0\frac{\partial v_0}{\partial x}\right)\left(v\ell_0(x)\Big|_{-1}^{1} - \int_{-1}^{1} v'\ell_0(x)dx\right) \\ &= \left(\alpha_-\tau_0 v_0 - \beta_-\tau_0\frac{\partial v_0}{\partial x}\right)\left(v_N\ell_0(x_N) - v_0\ell_0(x_0) - \sum_{i=0}^{N}\omega_i\frac{\partial v_i}{\partial x}\ell_0(x_i)\right) \\ &= \left(\alpha_-\tau_0 v_0 - \beta_-\tau_0\frac{\partial v_0}{\partial x}\right)\left(-v_0 - \omega_0\frac{\partial v_0}{\partial x}\right) \\ &= -\alpha_-\tau_0\left(v_0\right)^2 + \left(\beta_-\tau_0 - \alpha_-\tau_0\omega_0\right)v_0\frac{\partial v_0}{\partial x} + \beta_-\tau_0\omega_0\left(\frac{\partial v_0}{\partial x}\right)^2.\end{aligned}$$

The third term of right hand side

$$\begin{aligned}
\sum_{i=0}^{N}\tau_N\ell'_N(x_i)\left(\alpha_+v_N+\beta_+\frac{\partial v_N}{\partial x}\right)v_i\omega_i &= \alpha_+\tau_N v_N\int_{-1}^{1}v\ell'_N(x)dx+\beta_+\tau_N\frac{\partial v_N}{\partial x}\int_{-1}^{1}v\ell'_N(x)dx\\
&=\left(\alpha_+\tau_N v_N+\beta_+\tau_N\frac{\partial v_N}{\partial x}\right)\left(v\ell_N(x)\Big|_{-1}^{1}-\int_{-1}^{1}v'\ell_N(x)dx\right)\\
&=\left(\alpha_+\tau_N v_N+\beta_+\tau_N\frac{\partial v_N}{\partial x}\right)\left(v_N\ell_N(x_N)-v_N\ell_N(x_N)-\sum_{i=0}^{N}\omega_i\frac{\partial v_i}{\partial x}\ell_N(x_i)\right)\\
&=\left(\alpha_+\tau_N v_N+\beta_+\tau_N\frac{\partial v_N}{\partial x}\right)\left(-v_N-\omega_N\frac{\partial v_N}{\partial x}\right)\\
&=\alpha_+\tau_N\left(v_N\right)^2+\left(\beta_+\tau_N-\alpha_+\tau_N\omega_N\right)v_N\frac{\partial v_N}{\partial x}-\beta_+\tau_N\omega_N\left(\frac{\partial v_N}{\partial x}\right)^2.
\end{aligned}$$

Thus, the energy rate equation can be written as

$$\begin{aligned}
\frac{1}{2\nu}\frac{d}{dt}\sum_{i=0}^{N}v_i^2\omega_i =& v_N\frac{\partial v_N}{\partial x}-v_0\frac{\partial v_0}{\partial x}-\sum_{i=0}^{N}\left(\omega_i\frac{\partial v_i}{\partial x}\right)^2-\alpha_-\tau_0v_0^2+\left(\beta_-\tau_0-\alpha_-\tau_0\omega_0\right)v_0\frac{\partial v_0}{\partial x}\\
&+\beta_-\tau_0\omega_0\left(\frac{\partial v_0}{\partial x}\right)^2-\alpha_+\tau_Nv_N^2-\left(\beta_+\tau_N-\alpha_+\tau_N\omega_N\right)v_N\frac{\partial v_N}{\partial x}+\beta_+\tau_N\omega_N\left(\frac{\partial v_N}{\partial x}\right)^2\\
=&\frac{1}{2}\boldsymbol{V}_-^T\boldsymbol{A}_-\boldsymbol{V}_-+\frac{1}{2}\boldsymbol{V}_+^T\boldsymbol{A}_+\boldsymbol{V}_+-\sum_{i=1}^{N-1}\left(\frac{\partial v_i}{\partial x}\right)^2\omega_i.
\end{aligned}$$

For $\tau_\pm$ given by Eq. (11), $\boldsymbol{A}_\pm$ are semi-negative definite. Hence, we can ensure that the fully-discrete scheme is stable.

## B. Stability analysis of two-dimensional semi-discrete schemes

Assuming homogeneous boundary conditions, multiplying $v_{ij}\omega_{ij}$ to Eq. (12a) and summing all resultant collocation equations, we have the energy rate equation

$$\frac{1}{2\nu}\frac{d}{dt}\sum_{ij}^{MN}(v^2\omega)|_{ij}=\sum_{ij}^{MN}\left(\omega v\frac{\partial F_x}{\partial x}\right)\Big|_{ij}+\sum_{ij}^{MN}\left(\omega v\frac{\partial F_y}{\partial y}\right)\Big|_{ij}.$$

There has six term on the right hand side, we will discuss each one as follows, respectively.

The first term of right hand side

$$\begin{aligned}
\sum_{ij}^{MN}\left(v\omega\frac{\partial^2 v}{\partial x^2}\right)\Big|_{ij} &= \sum_{j=0}^{N}\omega_j^y\sum_{i=0}^{M}\left(\omega^x v_j\frac{\partial^2 v_j}{\partial x^2}\right)\Big|_i \\
&= \sum_{j=0}^{N}\omega_j^y\int_{x=-1}^{1} v_j\frac{\partial^2 v_j}{\partial x^2}dx \\
&= \sum_{j=0}^{N}\omega_j^y\left[\left(v_j\frac{\partial^2 v_j}{\partial x^2}\right)\Big|_{x=-1}^{1}-\int_{x=-1}^{1}\left(\frac{\partial^2 v_j}{\partial x^2}\right)^2 dx\right] \\
&= \sum_{j=0}^{N}\omega_j^y v_{Mj}\frac{\partial v_{Mj}}{\partial x}-\sum_{j=0}^{N}\omega_j^y v_{0j}\frac{\partial v_{0j}}{\partial x}-\sum_{ij}^{MN}\left[\left(\frac{\partial v}{\partial x}\right)^2\omega\right]\Big|_{ij}.
\end{aligned}$$

The second term of right hand side

$$\begin{aligned}
&\sum_{i=0}^{M}\sum_{j=0}^{N}\sum_{j'=0}^{N} v_{ij}\omega_{ij}\tau^{(a)}\frac{\partial}{\partial x}L_{0j'}(x_i,y_j)\left(\alpha^{(a)}v_{0j'}-\beta^{(a)}\frac{\partial v_{0j'}}{\partial x}\right) \\
&= \sum_{j=0}^{N}\sum_{j'=0}^{N}\omega_j^y\tau^{(a)}\ell_{j'}^x(y_j)\left(\alpha^{(a)}v_{0j'}-\beta^{(a)}\frac{\partial v_{0j'}}{\partial x}\right)\sum_{i=0}^{M}v_{ij}\omega_i^x\frac{\partial}{\partial x}\ell_0^x(x_i) \\
&= \sum_{j=0}^{N}\omega_j^y\tau^{(a)}\left(\alpha^{(a)}v_{0j}-\beta^{(a)}\frac{\partial v_{0j}}{\partial x}\right)\int_{x=-1}^{1}v_j d\left(\ell_0^x(x)\right) \\
&= \sum_{j=0}^{N}\omega_j^y\tau^{(a)}\left(\alpha^{(a)}v_{0j}-\beta^{(a)}\frac{\partial v_{0j}}{\partial x}\right)\left[\left(v_j\ell_0^x(x)\right)\Big|_{x=-1}^{1}-\int_{x=-1}^{1}\frac{\partial v_j}{\partial x}\ell_0^x(x)dx\right] \\
&= \sum_{j=0}^{N}\omega_j^y\tau^{(a)}\left(\alpha^{(a)}v_{0j}-\beta^{(a)}\frac{\partial v_{0j}}{\partial x}\right)\left(-v_{0j}-\sum_{i=0}^{M}\frac{\partial v_{ij}}{\partial x}\ell_0^x(x_i)\omega_i^x\right) \\
&= -\tau^{(a)}\alpha^{(a)}\sum_{j=0}^{N}(v_{0j})^2\omega_j^y+\tau^{(a)}\left(\beta^{(a)}-\alpha^{(a)}\omega_0^x\right)\sum_{j=0}^{N}v_{0j}\frac{\partial v_{0j}}{\partial x}\omega_j^y+\tau^{(a)}\beta^{(a)}\sum_{j=0}^{N}\left(\frac{\partial v_{0j}}{\partial x}\right)^2\omega_{0j}.
\end{aligned}$$

The third term of right hand side

$$\sum_{i=0}^{M}\sum_{j=0}^{N}\sum_{j'=0}^{N} v_{ij}\omega_{ij}\tau^{(b)}\frac{\partial}{\partial x}L_{Mj'}(x_i,y_j)\left(\alpha^{(b)}v_{Mj'}+\beta^{(b)}\frac{\partial v_{Mj'}}{\partial x}\right)$$

$$=\sum_{j=0}^{N}\sum_{j'=0}^{N}\omega_j^y\tau^{(b)}\ell_{j'}^x(y_j)\left(\alpha^{(a)}v_{Mj'}+\beta^{(b)}\frac{\partial v_{Mj'}}{\partial x}\right)\sum_{i=0}^{M}v_{ij}\omega_i^x\frac{\partial}{\partial x}\ell_M^x(x_i)$$

$$=\sum_{j=0}^{N}\omega_j^y\tau^{(b)}\left(\alpha^{(b)}v_{Mj}+\beta^{(b)}\frac{\partial v_{Mj}}{\partial x}\right)\int_{x=-1}^{1}v_j d\left(\ell_M^x(x)\right)$$

$$=\sum_{j=0}^{N}\omega_j^y\tau^{(b)}\left(\alpha^{(a)}v_{Mj}+\beta^{(b)}\frac{\partial v_{Mj}}{\partial x}\right)\left[\left(v_j\ell_M(x)\right)\Big|_{x=-1}^{1}-\int_{x=-1}^{1}\frac{\partial v_j}{\partial x}\ell_M^x(x)dx\right]$$

$$=\sum_{j=0}^{N}\omega_j^y\tau^{(b)}\left(\alpha^{(a)}v_{Mj}+\beta^{(b)}\frac{\partial v_{Mj}}{\partial x}\right)\left(v_{Mj}-\sum_{i=0}^{M}\frac{\partial v_{ij}}{\partial x}\ell_M^x(x_i)\omega_i^x\right)$$

$$=\tau^{(b)}\alpha^{(b)}\sum_{j=0}^{N}(v_{Mj})^2\omega_j^y+\tau^{(b)}\left(\beta^{(b)}-\alpha^{(b)}\omega_M^x\right)\sum_{j=0}^{N}v_{Mj}\frac{\partial v_{Mj}}{\partial x}\omega_j^y-\tau^{(b)}\beta^{(b)}\sum_{j=0}^{N}\left(\frac{\partial v_{Mj}}{\partial x}\right)^2\omega_{Mj}.$$

The $4^{th}$ term of right hand side

$$\sum_{ij}^{MN}\left(v\omega\frac{\partial^2 v}{\partial y^2}\right)\Big|_{ij}=\sum_{i=0}^{M}\omega_i^x\sum_{j=0}^{N}\left(\omega v_i\frac{\partial^2 v_i}{\partial x^2}\right)\Big|_j$$

$$=\sum_{i=0}^{M}\omega_i^x\int_{y=-1}^{1}v_i\frac{\partial^2 v_i}{\partial x^2}dx$$

$$=\sum_{i=0}^{M}\omega_i^X\left[\left(v_i\frac{\partial^2 v_i}{\partial x^2}\right)\Big|_{y=-1}^{1}-\int_{y=-1}^{1}\left(\frac{\partial^2 v_i}{\partial x^2}\right)^2dx\right]$$

$$=\sum_{i=0}^{N}\omega_i^x v_{iN}\frac{\partial v_{Nj}}{\partial x}-\sum_{i=0}^{M}\omega_i^x v_{i0}\frac{\partial v_{i0}}{\partial x}-\sum_{ij}^{MN}\left[\left(\frac{\partial v}{\partial x}\right)^2\omega\right]\Big|_{ij}.$$

The $5^{th}$ term of right hand side

$$\begin{aligned}
&\sum_{i=0}^{M}\sum_{j=0}^{N}\sum_{i'=0}^{M} v_{ij}\omega_{ij}\tau^{(c)}\frac{\partial}{\partial y}L_{i'0}(x_i,y_j)\left(\alpha^{(c)}v_{i'0}-\beta^{(c)}\frac{\partial v_{i'0}}{\partial x}\right)\\
&\quad=\sum_{i=0}^{M}\sum_{i'=0}^{M}\omega_i^x\tau^{(c)}\ell_{i'}^x(x_i)\left(\alpha^{(c)}v_{i'0}-\beta^{(c)}\frac{\partial v_{i'0}}{\partial y}\right)\sum_{j=0}^{N}v_{ij}\omega_j^y\frac{\partial}{\partial y}\ell_0^y(y_j)\\
&\quad=\sum_{i=0}^{M}\omega_i^x\tau^{(c)}\left(\alpha^{(c)}v_{i0}-\beta^{(c)}\frac{\partial v_{i0}}{\partial x}\right)\int_{y=-1}^{1}v_i d\left(\ell_0^y(y)\right)\\
&\quad=\sum_{i=0}^{M}\omega_i^x\tau^{(c)}\left(\alpha^{(c)}v_{i0}-\beta^{(c)}\frac{\partial v_{i0}}{\partial x}\right)\left[\left(v_i\ell_0^y(y)\right)\big|_{y=-1}^{1}-\int_{y=-1}^{1}\frac{\partial v_i}{\partial y}\ell_0^y(y)dy\right]\\
&\quad=\sum_{i=0}^{M}\omega_i^x\tau^{(c)}\left(\alpha^{(c)}v_{i0}-\beta^{(c)}\frac{\partial v_{i0}}{\partial x}\right)\left(-v_{i0}-\sum_{j=0}^{N}\frac{\partial v_{ij}}{\partial y}\ell_0^y(y_j)\omega_j^y\right)\\
&\quad=-\tau^{(c)}\alpha^{(c)}\sum_{i=0}^{M}(v_{i0})^2\omega_i^x+\tau^{(c)}\left(\beta^{(e)}-\alpha^{(c)}\omega_0^y\right)\sum_{i=0}^{M}v_{i0}\frac{\partial v_{i0}}{\partial y}\omega_i^x+\tau^{(c)}\beta^{(c)}\sum_{i=0}^{M}\left(\frac{\partial v_{i0}}{\partial y}\right)^2\omega_{i0}.
\end{aligned}$$

The $6^{th}$ term of right hand side

$$\begin{aligned}
&\sum_{i=0}^{M}\sum_{j=0}^{N}\sum_{i'=0}^{M} v_{ij}\omega_{ij}\tau^{(d)}\frac{\partial}{\partial y}L_{i'N}(x_i,y_j)\left(\alpha^{(d)}v_{i'N}+\beta^{(d)}\frac{\partial v_{i'N}}{\partial x}\right)\\
&\quad=\sum_{i=0}^{M}\sum_{i'=0}^{M}\omega_i^x\tau^{(d)}\ell_{i'}^x(x_i)\left(\alpha^{(d)}v_{i'N}+\beta^{(d)}\frac{\partial v_{i'N}}{\partial y}\right)\sum_{j=0}^{N}v_{ij}\omega_j^y\frac{\partial}{\partial y}\ell_N^y(y_j)\\
&\quad=\sum_{i=0}^{M}\omega_i^x\tau^{(d)}\left(\alpha^{(d)}v_{iN}+\beta^{(d)}\frac{\partial v_{iN}}{\partial x}\right)\int_{y=-1}^{1}v_i d\left(\ell_N^y(y)\right)\\
&\quad=\sum_{i=0}^{M}\omega_i^x\tau^{(d)}\left(\alpha^{(d)}v_{iN}+\beta^{(d)}\frac{\partial v_{iN}}{\partial x}\right)\left[\left(v_i\ell_N^y(y)\right)\big|_{y=-1}^{1}-\int_{y=-1}^{1}\frac{\partial v_i}{\partial y}\ell_N^y(y)dy\right]\\
&\quad=\sum_{i=0}^{M}\omega_i^x\tau^{(d)}\left(\alpha^{(d)}v_{iN}+\beta^{(d)}\frac{\partial v_{iN}}{\partial x}\right)\left(v_{iN}-\sum_{j=0}^{N}\frac{\partial v_{ij}}{\partial y}\ell_N^y(y_j)\omega_j^y\right)\\
&\quad=\tau^{(c)}\alpha^{(d)}\sum_{i=0}^{M}(v_{iN})^2\omega_i^x+\tau^{(d)}\left(\beta^{(d)}-\alpha^{(d)}\omega_N^y\right)\sum_{i=0}^{M}v_{iN}\frac{\partial v_{iN}}{\partial y}\omega_i^x-\tau^{(d)}\beta^{(d)}\sum_{i=0}^{M}\left(\frac{\partial v_{iN}}{\partial y}\right)^2\omega_{iN}.
\end{aligned}$$

Thus, the energy rate equation can be written as

$$\begin{aligned}
\frac{1}{\nu}\frac{d}{dt}\sum_{ij}^{MN}(v^2\omega)|_{ij}\leq&\sum_{j=0}^{N}\omega_j^y(\boldsymbol{V}^{(a)})_j^T\boldsymbol{A}^{(a)}\boldsymbol{V}_j^{(a)}+\sum_{j=0}^{N}\omega_j^y(\boldsymbol{V}^{(b)})_j^T\boldsymbol{A}^{(b)}\boldsymbol{V}_j^{(b)}\\
&+\sum_{i=0}^{M}\omega_i^x(\boldsymbol{V}^{(c)})_i^T\boldsymbol{A}^{(c)}\boldsymbol{V}_i^{(c)}+\sum_{i=0}^{M}\omega_i^x(\boldsymbol{V}^{(d)})_i^T\boldsymbol{A}^{(d)}\boldsymbol{V}_i^{(d)}.
\end{aligned}$$

For $\tau^{(\gamma)}$ given by Eq. (15), $\boldsymbol{A}^{(\gamma)}$ are semi-negative definite. Hence, we can ensure that the fully-discrete scheme is stable.

## C. Stability analysis for penalty parameter $\tau$

Let $\lambda$ be the eigenvalue of the matrix function $\boldsymbol{A}$, and the characteristic polynomial of $\boldsymbol{A}$ is

$$\lambda^2 + 2\left(\alpha\tau + \omega(1-\beta\tau)\right)\lambda + 4\alpha\tau\omega(1-\beta\tau) - (1+\alpha\tau\omega-\beta\tau)^2 = 0. \tag{27}$$

Let $\lambda_1$ and $\lambda_2$ be the roots of above equation, and we can get

$$\lambda_1\lambda_2 = 4\alpha\tau\omega(1-\beta\tau) - (1+\alpha\tau\omega-\beta\tau)^2 \tag{28a}$$

$$= -\left((\alpha\omega+\beta)\tau - 1\right)^2, \tag{28b}$$

and

$$\lambda_1 + \lambda_2 = -2\left(\alpha\tau + \omega(1-\beta\tau)\right) \tag{29a}$$

$$= -2((\alpha-\beta\omega)\tau + \omega). \tag{29b}$$

For stability, we need $\lambda_1 \leq 0$ and $\lambda_2 \leq 0$. One can obtain $\lambda_1\lambda_2 \geq 0$, and $\lambda_1 + \lambda_2 \leq 0$. From Eq. (28b), we can get

$$\tau = \frac{1}{\alpha\omega+\beta}. \tag{30}$$

Then we check that for $\tau$ defined as Eq. (30)

$$\lambda_1 + \lambda_2 = -2((\alpha-\beta\omega)\tau + \omega) \tag{31a}$$

$$= -2\frac{\alpha+\alpha\omega^2}{\alpha\omega+\beta} < 0, \tag{31b}$$

indicating that $\boldsymbol{A}$ is semi-definite matrix.